Journal of Power Sources xxx (xxxx) 235221

Contents lists available at ScienceDirect

Journal of Power Sources

journal homepage: www.elsevier.com/locate/jpowsour

Review article

Gel polymer electrolyte composites in sodium-ion batteries: Synthesis methods, electrolyte formulations, and performance analysis

Farooq Ahmad [a,*], Amir Shahzad [b], Saira Sarwar [c], Hina Inam [d], Umer Waqas [e], Dawid Pakulski [c], Michal Bielejewski [a], Shahid Atiq [e,**], Sania Amjad [f], Muhammad Irfan [e], Hadia Khalid [e], Muhammad Adnan [e], Osama Gohar [g]

[a] Institute of Molecular Physics, Polish Academy of Sciences, M. Smoluchowskiego 17, 60-179, Poznań, Poland
[b] Institute of Physics, The Islamia University of Bahawalpur, Bahawalpur, 63100, Pakistan
[c] Centre for Advanced Technologies, Adam Mickiewicz University, Uniwerystetu Poznańskiego 10, Poznań, 61-614, Poland
[d] Department of Material Science and Technology, Parma University, Italy
[e] Centre of Excellence in Solid State Physics, University of the Punjab, Lahore, Pakistan
[f] Department of Chemistry, Government College Women University Sialkot, Pakistan
[g] Department of Chemistry, Hazara University, Mansehra, 21300, Khyber Pakhtunkhwa, Pakistan

ARTICLE INFO

Keywords:
Gel polymer electrolytes
Sodium-ion batteries
Electrochemical
Energy storage
Solid electrolytes

ABSTRACT

Gel polymer electrolytes (GPEs) are prevalent in battery research because they are flexible, lightweight, and promote reasonable contact between components. Sodium-ion batteries (NIBs) are gaining recognition as promising options for future energy storage due to their cost-effectiveness and environmental friendliness. To enhance safety, replacing traditional organic electrolytes with polymer electrolytes can prevent issues like thermal instability and electrolyte leakage. Polymer electrolytes (PEs) face high interfacial impedance and low ionic conductivity. GPEs offer a solution by balancing high ionic conductivity, thermal stability, low interfacial impedance, and flexibility. This review article discusses various methods for synthesizing GPEs and compares electrolytes for NIBs. It also highlights recent cathode and anode-material advancements, supported by schematic illustrations for clarity. Additionally, the article examines GPE composites for their electrochemical properties through a detailed analysis. This review could provide a thorough comprehension of sodium-ion GPEs and help shape how molecules interact to improve the performance of gel polymers NIBs.

1. Introduction

Currently, humanity faces two major issues: energy and the environment. Renewable and clean energy advancement is critical to human society's sustainable growth. Therefore, shifting from carbon-based hydrocarbons to renewable resources is a vital and effective way to maintain carbon neutrality and ensure an eco-friendly environment. Renewable resources like wind, solar, and tidal energy are utilized to alleviate environmental issues and air pollution. Although these renewable resources are beneficial for us due to intermittency and dependency on external conditions, there is a need for alternative energy storage systems to supply consumers with continuous and reliable energy that would meet their day-to-day energy demands. For that purpose, the production of wide-ranging electrochemical energy storage devices (ESDs) are developed to integrate renewable energy into the grid. In recent years, due to the expeditious demand for energy in electronics, convenient devices, and electrical energy storage, secondary stationary energy devices have been developed to make highly efficient ESDs [1,2]. In 1991, Sony Corporation introduced the initial commercially available lithium-ion battery (LIB) because of the pioneering work of three Nobel laureates in rechargeable LIBs. There are specific merits of LIBs, such as the ability to recharge, exhibit a high voltage, an excellent energy density (ED), and a low self-discharge rate. However, due to rapidly expanding demands of LIBs in 2015, restricted reserves, and the skyrocketed price of Li salt in 2021 made the researcher work on alternative secondary batteries with abundant resources such as sodium, being the fourth element in the earth's crust, NIBs which have high-voltage windows and high ED as differentiate to LIBs, both have similar

* Corresponding author.
** Corresponding author.
E-mail addresses: farooq.ahmad@ifmpan.poznan.pl (F. Ahmad), satiq.cssp@pu.edu.pk (S. Atiq).

https://doi.org/10.1016/j.jpowsour.2024.235221
Received 19 June 2024; Received in revised form 8 August 2024; Accepted 9 August 2024
0378-7753/

chemistry. The redox potential of sodium $\left(E\frac{Na+}{Na} = -2.71V\right)$ is similar to lithium $\left(E\frac{Li+}{Li} = -3.04V\right)$ [3,4].

The optimal functioning of high-performance rechargeable NIBs heavily depends on the electrolyte, playing a pivotal role in enabling the mobility of Na^+ ions while impeding electron diffusion [5]. Electrolytes are an essential part of the battery system and may be broadly classified into three major groups: liquid electrolytes (LEs), solid electrolytes (SEs), and GPEs. Most NIBs often use LEs, and the main advantage of LE is that they exhibit high conductivity (>0.001 S cm^{-1}) and a good connection with the electrode material. While, incorporating LEs in NIBs introduces the potential hazards of leaks and fires, especially when overcharging or abusive operations occur within electric vehicle applications [6,7]. To solve the problems mentioned above, SEs can be used to meet the requirements. Numerous researchers are actively addressing this challenge, emphasizing the substitution of traditional LEs with solid-state alternatives. Despite substantial mechanical strength, the SE detrimentally affects battery performance due to elevated electrode–electrolyte interconnected impedance and insufficient ionic conductivity. Because of their increased heat resistance, broader electrochemical window, and less risk of electrolyte outflow, GPEs are superior to LEs in LIBs/NIBs [8].

They are further categorized into SPE and GPEs. Furthermore, considering the variety of electrolytes that are accessible, classifying them as SPEs and GPEs alone may be restrictive. A broader categorizing would offer a more comprehensive outlook on the alternatives and advancements in electrolyte technology. In contrast to SPE, GPEs address these issues by amalgamating the advantages of both liquid and SEs; these GPEs provide increased ionic conductivity, low interfacial impedance, and the incorporation of inorganic electrolyte fillers provide high thermal stability and flexibility [9]. GPEs comprise three groups, namely conductive ions, polymers, and plasticizers. For NIBs, sodium salt is the primary facilitator of Na^+ ion movement within the gel matrix. The polymer electrolyte with a plasticizer also increases ionic conductivity in normal conditions [10]. In the GPE, the plasticizers and conductive salt are the same as in LEs and these are merged between the polymer matrix that is converted into a flexible gel material [11]. The compounds that play the role of SEs are PVDF and its copolymer PVDF-co-hexafluoropropylene (PVDF-HFP) and poly (acrylonitrile-co-methyl acrylate) (PVDF-P(AN-co-MMA), and (PMMA) poly(methyl methacrylate), (PAN) polyacrylonitrile, (PEO) poly(ethylene oxide). Most research has been done on (PVDF-HFP) because of its excellent characteristics, like high ionic conductivity and reduced leakage and flammability because of no free-moving solvent, and both materials act as single materials [12]. GPEs could be tailored because of having different variety of compounds by changing the proportion of components, such as the number of polymers, plasticizers, and binary and tertiary solvents [13], in some cases by crosslinking of the polymer matrix [14], inserting the inorganic inert fillers. These modifications have profound effects on morphologies and mechanical and thermal properties. The anticipated output is the improvement of ionic conductivity as an electrochemical window; these modifications marked an impact on the battery conduction process. Consequently, the dimensional stability is accomplished, and the toxicity and flammability are reduced, and all of these variations guarantee improved safety for the electrolyte and the battery. The evaluation criteria for GPEs, depending on the polymer host, are illustrated in Fig. 1(b).

Fig. 1(b) shows typical kinds of GPEs but still have some distance from the ideal system. Therefore, various techniques have been devised based on advanced GPE systems to fulfill practical applications and the incorporation of nanofillers into GPEs, flame retardant GPE, and composite GPEs to boost the mechanical properties, ionic conductivity, and interfacial strength and safety of GPEs. Composite GPE came into existence to overcome the issue of poor mechanical strength. Composite GPE with another membrane can address these concerns.

1.1. History of GPEs and NIBs

Feuillade developed a GPE for Li–CuS batteries using PVP and PAN as polymer matrices and incorporating propylene carbonate (PC) as plasticizers. The initial research was started in 1975 on GPE for LIBs. However, this GPE type needed decent mechanical strength and elevated ionic conductivity. This remained unchanged until 1990 [15]. Abraham cited this work that the LIB GPE has the plasticizer constituted of PC and EC, with ionic conductivity reaching up to 0.001 S cm^{-1} level. The significant advantage of better mechanical properties and having free-standing films is due to the high dielectric

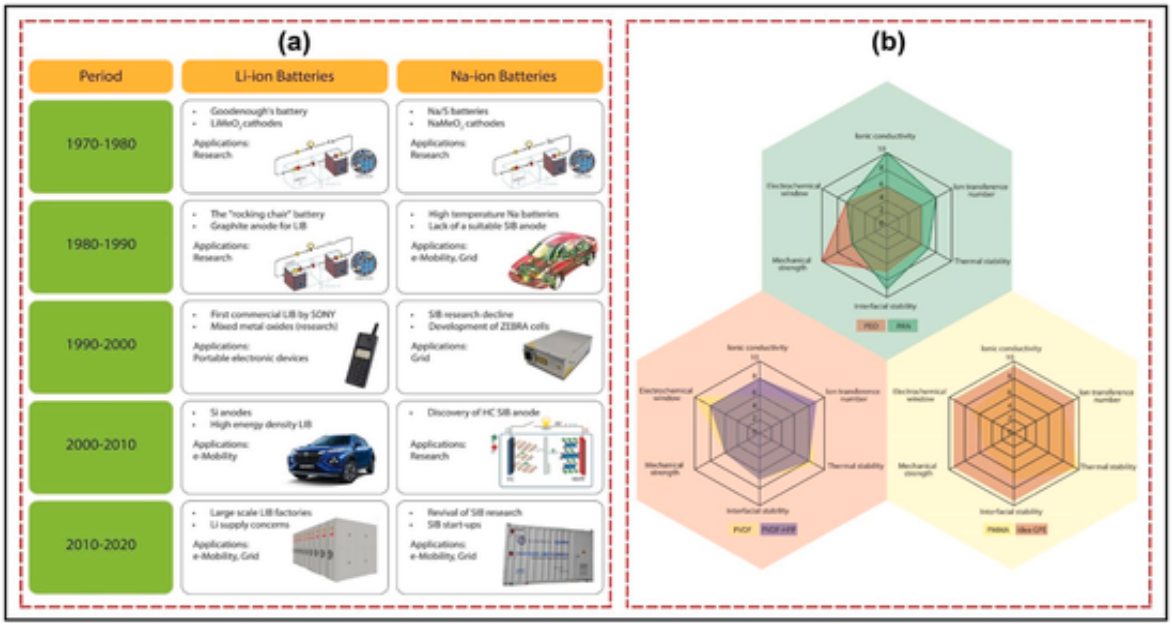

Fig. 1. (a) Evolution and driving factors in different decades: A comparative history of LIB and SIB **(b)** Evaluation criteria for GPEs based on the polymer host.

constants of PC and EC; moreover, adding a plasticizer, even in small proportion, can significantly enhance ionic conductivity. Hence, there is no need for a high amount of plasticizer for better solubility in PC/EC solution because PVDF has polar groups. In 1996, Tarson et al. worked on the manufacturing steps and operational outcomes of soft-pack GPE batteries commercialized by Bellcore/Telcordia. The batteries feature GPEs exhibiting positive mechanical and elastic attributes and a remarkable ionic conductivity of 3×10^{-3} S cm^{-1}. These GPEs comprise a polymer matrix incorporating PVDF-HFP and LEs of 60 % 1 M $LiPF_6$ in either EC/PC or EC/DMC solution [16].

On the other hand, Fig. 1(a) depicts the shared history of NIB and LIB from 1970 to 2020s. Goodenough constructed the first LIB in the 1970s to overcome the issues at the cathode side, and the chemical composition was $LiMeO_2$ for research applications [17]. Delmas and his co-workers reported the discovery of NIBs, $NaMeO_2$, in the early 1980s [18]. Then metallic lithium and sodium were used for the anode, but due to their electropositive, they reacted with electrolytes and caused instability and dendrite growth. This prompted the development nature of the rocking chair battery proposed by Scrosati. Yazami and Touzain found that soft carbon anode or graphite can be used because of its capability to intercalate lithium at high gravimetric capacity and low voltage. By this research, Yoshino was capable of making carbon anode and $LiCO_2$ anode, and this was the first commercialized by Sony in 1991 [19]. Unfortunately, carbonaceous materials are not effective in the case of NIBs as anode this posed a significant obstacle and emerged as another major hindrance to the commercial potential of NIBs. In the following years, from the 1990s to the 2000s, there was a sharp decline in NIBs. Despite declining research in NIBs, the first cell was developed by Zeolite Battery Research Africa (ZEBRA), which was operated at low temperatures [20]. The areas of applications are e-mobility, energy storage, and space missions. In the 2000s, Stevens and Dahn discovered sodium intercalation into hard carbons (HC), which led to an interest in room-temperature NIB. HC anode has better properties as compared to LIBs [21].

Since 2010 NIB cathode material has had unparalleled advancement. To achieve energy arbitrage through load shifting, HiNa announced in April 2019 the construction of the most extensive NIB module—a 100,000 Wh (30,000 W power) battery installation in the Chinese city of Liyang [22].

2. Effect of porous GPEs on NIBs performance

The performance of NIBs is influenced by porosity, which plays a critical role, particularly in the context of GPEs. While porosity in electrode materials significantly affects ion diffusion kinetics, structural stability, and overall electrochemical performance, it is equally important to highlight the role of porosity in GPEs. The porosity of GPEs directly affects the electrolyte absorption rate and ionic conductivity, which are critical for the efficient functioning of NIBs. Greater porosity often enables faster ion transport, leading to more enormous pore volumes and increased surface area. This increases the battery's power density and enhances its rate capabilities [23]. Reduced battery performance and poor electrode-electrolyte contact can arise from inadequate porosity, which can cause an uneven electrolyte distribution. Porosity and its importance in the context of NIB is shown in Fig. 2.

An ultrathin polymer fibrous membrane with pores was fabricated [24]. The main reason for increased electrochemical stability is the large surface area of electrospun polymer and interconnected pores [25].

2.1. Electrolyte absorption rate

The electrolyte absorption rate measures how well the electrolyte can infiltrate and saturate the GPE. Proper porosity in GPEs ensures that the LE can penetrate the polymer matrix thoroughly, maximizing contact with the active area for enhanced performance. This thorough saturation is vital because it allows for efficient ion transport throughout the electrolyte, which is necessary for maintaining high electrochemical performance.

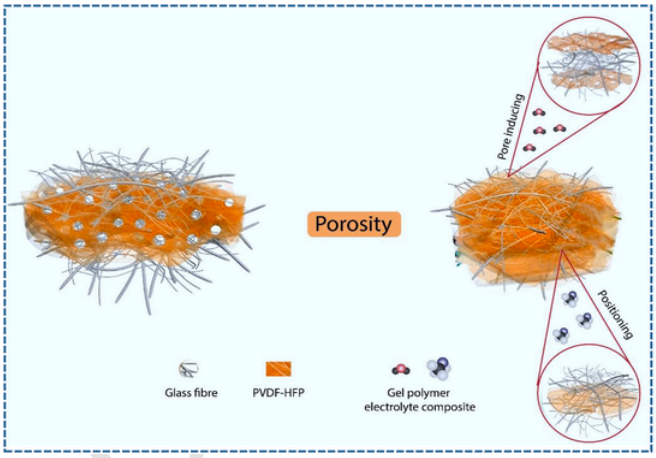

Fig. 2. Porosity and its importance for the GPE Sodium Ion battery.

GPEs with higher porosity can absorb more electrolytes, resulting in better ionic conductivity and improved battery performance. Inadequate porosity, on the other hand, can lead to poor electrolyte penetration, uneven distribution, and reduced battery efficiency. Ensuring optimal porosity in GPEs helps maintain uniform electrolyte distribution, facilitating smooth and efficient ion transport.

2.2. Ionic conductivity

It is a critical parameter that dictates the speed at which ions traverse through the electrolyte. High ionic conductivity is essential for rapid charge-discharge cycles and overall battery efficiency. The porosity of GPEs plays a significant role in enhancing ionic conductivity. A higher porosity provides more pathways for ion transport, reducing the resistance ions face moving through the electrolyte.

The fabrication method of GPEs, such as electrospinning, can significantly influence their porosity. For instance, the electrospinning method creates ultrathin polymer fibrous membranes with interconnected pores. These pores increase the surface area and provide maximum inner space between the electrospun fibers, facilitating rapid ion movement. Aleksandar et al. demonstrated that polyacrylonitrile (PAN)--based GPE fabricated via electrospinning improved capacity and reduced overvoltage polarization in room-temperature Na–S batteries. This improvement is attributed to the high uptake of the LE, resulting from the greater porosity and enhanced ionic conductivity.

2.3. Electrochemical stability

The electronic properties of functional groups and chain structures contribute to their broad electrochemical and thermal stability; however, to some extent, the large surface areas and interconnected pores of electrospun polymer membranes also contribute. These result in better electrolyte absorption, higher ionic conductivity, and stable cyclic performance. This is crucial for the longevity and reliability of NIBs, as it ensures that the battery can maintain its performance over numerous charge-discharge cycles.

In wrap-up, the porosity of GPEs is a critical factor that significantly influences the performance of NIBs. It influences the electrolyte absorption rate and ionic conductivity, which are crucial for efficient ion transport and overall battery performance. Optimizing the GPEs porosity can enhance the electrochemical stability, power density, and rate

capabilities of NIBs, leading to more efficient and durable battery systems.

3. An operational mechanism in NIB

NIB cells consist of a cathode composed of a sodium-based material, an anode (which may or may not be sodium-based), and an LE that contains sodium salts that have dissociated in polar protic or aprotic solvents [26,27]. During the charging process, Na^+ transfers from the cathode to the anode. Concurrently, electrons traverse the external circuit. During the discharge process, an opposite process takes place, as shown in Fig. 3(b).

The operational mechanism of NIBs is analogous to that of LIBs, involving the process of Na-ion embedding and stripping between cathode and anode to facilitate charging and discharging [28–30]. During charging, Na^+ ions are removed from the positive electrode material and introduced into the electrolyte to the harmful electrode material. Electrons move from the external circuit to the negative terminal to maintain charge equilibrium. In contrast, Na^+ ions are removed from the cathode and transferred via an electrolyte to the electrode. The addition and removal of Na^+ between the positive and negative electrodes during the standard charging and discharging process does not affect the electrode's material's primary chemical composition. Sodium's ionic state is maintained throughout the removal and inserting processes. Na^+ may induce a swing at the anode and cathode of the battery, sometimes known as the "*Rocking chair battery*" [31].

One of the critical characteristics of NIBs is the replacement of Na^+ for the expensive Li^+. For the proper functioning of the NIB, changes to the electrolyte, positive, and negative charges are necessary. The NIB may discharge zero volts since it does not have over-discharge characteristics. Comparable to lithium iron phosphate batteries, NIBs have an ED of more than 100 Wh/kg. Moreover, it offers a distinct practical benefit and might replace a conventional lead-acid battery for specific energy storage uses. A series of materials for the anode and cathode have been improved since 2010 by the unique characteristics of the NIB, leading to significant improvements in capacity and cycle life [32]. Negative electrodes are made of HC, transition metals, or alloys of these metals. Positive electrodes, such as polyanionic, Prussian blue, and oxide materials, particularly Na_xMO_2 with a layered structure and binary and ternary materials, have excellent specific capacity for charge-discharge and cycle stability [33–37].

3.1. Components of NIB

NIB is similar to a LIB regarding basic structure; the only difference is the kind of ions used for charge transfer. Both types of batteries employ electrical storage. The intercalation chemistry of sodium in cathode material is similar to that of lithium, enabling the use of chemically analogous substances in both systems. Nonetheless, these systems are distinct from one another. The radii of the Na^+ ions is 1.02 *Å*, relatively more significant than the size of Li^+ ions, which is 0.76 *Å* [37,38]. This size disparity is significant in terms of phase stability, transport characteristics, and the development of interphases. With a mass of 23 g mol^{-1}, sodium is heavier than lithium, which weighs 6.9 g mol^{-1}.

In comparison, lithium, which has an electrode potential of 3.02 V, exhibits a more significant potential of 2.71 V when measured against standard hydrogen potential. Thus, NIB-decreased ED will be a constant property. Nevertheless, cyclic Li^+ or Na^+ constitutes only a tiny fraction of the total component weight. On the other hand, the capacity is primarily dictated by the properties of the host materials used for the electrodes [39].

3.2. Binders for NIBs

Physical and chemical bonding are the two main ways binders form connections. Binders can be mechanically attached to electrode materials for a solid binding effect by embedding, interconnecting, or other means, which is the primary basis of physical bonding. Basic types of chemical bonds, including molecular forces, hydrogen bonds, covalent bonds, and coordination bonds, can form an unbroken bonding network between the material and the polymer binder. Just recently, there has been some focus on how to optimize the working of NIB binders in terms of self-healing, multifunctionality, high electron/ion conductivity, strong bonding, and so on. Recently, for cathode as well as for anode materials, several different types of binders in NIBs have been reported simultaneously [40]. As one of the more traditional polymer binders, PVDF may be classified as oil-based or water-based depending on the solvent's characteristics; NMP is by far the most common solvent. The oil-soluble PVDF material is mainly utilized as a cathode binder, and its excellent electrochemical stability has led to its extensive usage as an oil-based binder in the fabrication of electrodes for battery systems.

The literature indicates that cathode binders can use an oily system up to 90 % of the time, with water-soluble binders accounting for

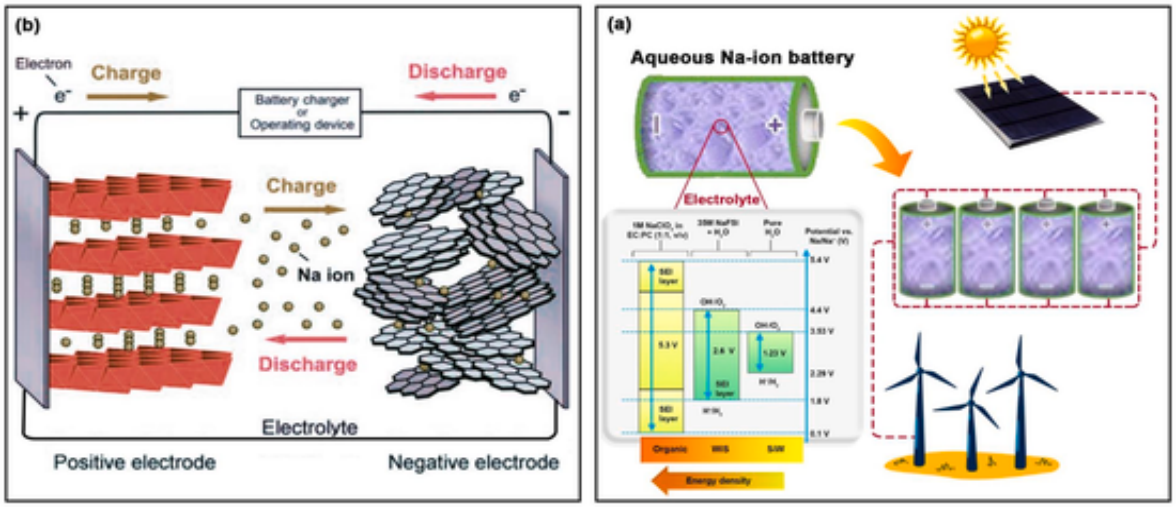

Fig. 3. (a) Schematic diagram of aqueous electrolyte in Na-ion battery **(b)** Schematic diagram of the operational mechanism of the sodium ion battery.

around 10 % of the time. This is because water-based solvents like sodium vanadium phosphate can damage almost every cathode material, and Prussian blue may readily absorb water and harm the structure. The systems that utilize water are more challenging to dry than those that use oil, and any remaining moisture can diminish the battery's cycling performance and storage capacity. In contrast, anode electrodes that use a water-based binder are more common since they are less likely to cause environmental damage and can lessen polarization [41–43]. However, the battery's capacity will decrease due to an increase in internal polarization caused by using the PVDF binder. Amorphous polyacrylic acid (PAA) has several carboxyl functional groups and an extended carbon chain structure, allowing it to create strong hydrogen bonds with binders, current collectors, and active materials. Electrode materials often contain a PAA binder, which is electrochemically inert and does not undergo any side reactions when charged or discharged. After the volume expands due to Na^+ intercalation/deintercalation during cycling, the structure's hydrogen bonds allow the electrode to return to its previous size and re-establish a new conductive network.

A polymer formed from brown algae that occurs naturally, sodium alginate (SA) is an integral part of an electrode. Because of its abundance of hydroxyl and carboxyl groups, the protonation of SA makes it an excellent hydrogen bond facilitator. When applied to porous materials, the SA binder may patch up surface imperfections, increasing initial coulombic efficiency while decreasing SEI film consumption. SA binder might be a good fit for materials to improve the cycle stability of electrode materials that can esterify with the carboxyl group for NIBs. The natural polyanionic polysaccharide molecule carboxymethyl cellulose (CMC) has a long-chain structure with numerous carboxymethyl and hydroxyl groups and is generated from cellulose. These functional groups can enhance the bonding performance by forming chemical connections with active materials. Electrode materials with a CMC binder outperform those with a typical PVDF binder in electrochemical performance for NIBs [44–49]. Evidence suggests that conventional binders like PVDF, PAA, SA, and CMC can form strong bonds, keeping the electrode structure intact and prolonging the battery's cycle life.

Further development of high-performance NIBs still needs to be improved by traditional binders' weak self-healing capabilities and limited electron/ion conduction; hence, a new conductive-type binder must be designed. In this context, Yang et al. discovered that a very effective conductive binder may be made by reacting polyfluorene (PF) polymers along methyl benzoic ester-$PhCOOCH_3$ and carbonyl C = O group. It is possible to enhance the LUMO electronic states and adhesion of polymer binder by function groups, including carbonyl C = O and methyl benzoic ester-$PhCOOCH_3$. The significant volume expansion of the Sn electrode during charging and discharging could be minimized by employing PFFOMB as a conductive binder of NIBs, leading to an improvement in electrochemical performance that surpasses that of conventional PVDF and CMC binders.

3.3. Anode materials for NIBs

The traditional anode materials graphite and silicon, for LIBs, have a limited ability to store Na; finding suitable anodes for NIBs has been an uphill battle. Due to its modest melting point of 97.7 °C and its tendency to develop dendrites [50], which would present security difficulties, as an anode for a Na metal system, even metallic sodium is ineligible. Possible anodes for Na-ion systems can be made of various materials, including compounds that store sodium by insertion, alloying, intercalation, or conversion processes. These potential anode materials comprise organic compounds such as carbonyls, Schiff bases, or Quinone derivatives. There is also the possibility of using inorganic oxides such as $Na_2Ti_3O_7$, Co_3O_4, CuO, or Fe_2O_3 for intercalation or conversion. Possible additional elements contain disordered carbons and elements (Sb and P) from groups 14 and 15 that alloy with sodium [51]. An in-depth analysis of the first group of materials demonstrates that the high molar mass of oxide-based materials, like Na(Fe, Ti)O_4 or $Na_2Ti_3O_7$, causes them to have a less specific capacity. However, their exceptional stability stems from their inorganic scaffold, which results in excellent cycling performance. Anodes made of several types of TiO_2 have also been investigated, including anatase, rutile, or β-TiO_2. They are also classified as commercial NIBs, albeit with a low specific capacity. Organic electrodes were developed to address this problem [52]. Although there are several benefits to using organic anodes, such as their inexpensive cost, an abundance of resources, high capacity, and a great deal of structural flexibility—they also have some undesirable traits, such as pulverization both when the cycling and breakdown of organic molecules in the electrolyte and low electrical conductivity. By improving the composite electrode's conductivity and attaching the organic molecules, additions like graphene can reduce these adverse effects. Additives can be used for surface modification and counteract organic compound dissolution, and salt creation, encapsulation, polymerization, and electrolyte choice are other options to consider. There have been encouraging early findings from the creation of organic NIBs. Researchers are looking at carbon-based compounds like graphene or amorphous carbons as potential solutions to the problem of capacity loss caused by cycling. Graphite is not a significant candidate among carbon-based materials since it does not absorb much sodium when using regular electrolytes; Na^+ ions can only be reversibly intercalated into graphite using glyme-based electrolytes.

Conversely, achieving anode materials with a higher specific energy requires immediate attention to two pressing issues: the poor coulombic efficiency and the need to reduce the operating voltage. Regardless, the precursors and the synthetic circumstances are the deciding factors in producing carbon with a specific microstructure, microporosity, and surface area, all of which govern the material's electrochemical performance. Optimizing all these factors would be very beneficial from a sustainability and economic perspective for a worldwide market for grid-energy storage.

3.4. Cathode materials for NIBs

The chemically diverse range of materials that can serve as Na-ion channel cathodes includes many unique families. Consequently, the vast variety of materials capable of reversible Na^+ extraction/insertion stabilizes a broad range of functional configurations because of the size difference between transition metal ions and Na^+ ions. In Polyanionic compounds (e.g., phosphates, fluorophosphate, mixed phosphates), Prussian blue derivatives (PBAs), organic compounds such as redox-active polymers or conjugated carbonyls and transition metal fluorides or oxyfluorides are the primary families of materials investigated for use as Na-ion cathodes [53,54]. Among the mentioned cathode materials, polyanionic compounds, and layered transition metal oxides are the most promising. For several reasons, including their scalable synthesis, low cost, origin from earth-abundant precursors, and outstanding electrochemical performance, Na-layered oxide cathodes are preferred in NIBs. Several recent review articles provide insightful analyses of the current understanding of sodium layered oxide cathodes and their evolution. When considering the electrochemical properties of Na_xMO_2 compounds, the two most intriguing structures are the P_2- and O_3-phases, distinguished by the relative placement of the transition metal layer and Na^+.

Some potential cathode materials that undergo conversion processes with sodium include oxyfluorides, sulfides (Fe_xS_y, Co_xS_y), selenides, transition metal fluorides (MF_x, where M = Ni, V, Cu, Ti, Fe, and Co; and x = 2 or 3), or even CuCl and $CuCl_2$ [30–36]. These materials would be ideal for building high-performance NIBs since, in theory, their specific capacity (C_{sp}) and, thus, energy densities are far higher than those of materials based on intercalation processes. However, their sluggish Na^+ diffusion, high over potential during electrochemical re-

actions, and considerable volume change are significant drawbacks that they still face today. We still have a ways to go before we can optimize conversion-based cathodes or NIBs for practical usage. However, several solutions that might help us overcome these limitations are being studied. The availability of materials, molar mass, less expense, safety, structural adaptability, mechanical flexibility, and absence of a transition metal have all played a role in the organic positive electrode status as a potentially promising alternative cathode material for NIBs. These characteristics make NIBs more pliable, lightweight, and portable. In particular, the creation of organic batteries that are both renewable and ecologically friendly has been the primary emphasis of research on organic NIBs. Scientists are investigating various materials, including organosulfur compounds, carbonyl compounds (such as PTCDA and disodium rhodizonate), organic radical compounds, and conducting polymers. Recent research on organic electrodes has focused on the carbonyl compound family. However, there are still unanswered questions about these materials. The primary issues with these systems include cathode dissolution in the electrolyte, which results in fast capacity fading, low electronic conductivity leading to low rate performance, and high energy density cathodes due to increased working potentials of the electrodes. The three groups of materials examined demonstrate experimental C_{sp} values ranging from 100 to 200 mAh g^{-1}, rendering them appropriate for use as cathodes in commercial NIBs. These groups are layered oxides, polyanionic compounds, and PBAs [55].

4. Electrolytes for NIBs

Currently, carbonates are used as the organic solvent, and $NaPF_6$ or $NaClO_4$ as the Na salt in NIBs. These type of electrolytes have shown outstanding overall performance with various NIB-positive and harmful materials. The metal sodium electrode is susceptible to corrosion from this electrolyte over extended periods of operation. Because of this, the battery's electrochemical performance drops, and the SEI membrane becomes less stable. Furthermore, LEs often provide possible safety risks, including the possibility of liquid leakage and combustion. Emphasizing the electrode process interface is crucial when working with the well-established LEs of NIB. This will enhance safety and increase reliability with the materials used for electrodes and battery accessories [56–59].

4.1. Requirements for a suitable electrolyte in Na ion battery

NIBs require electrolytes that fulfill several essential requirements. First, they ought to successfully lower internal cell resistance and minimize resistive heating by increasing ionic conductivity. Moreover, the chemical stability of the electrolyte solvents on the surfaces of strongly reducing anode materials is essential to halting degradation. The electrochemical stability of the electrode materials plays a critical role in maintaining a high voltage differential and preventing side reactions. The electrolyte material should also have a low melting point to guarantee sufficient conductivity at temperatures lower than ambient. This will stop solidification and phase separation. High boiling temperatures are required to stop internal pressure from building up and material evaporation. Finally, for practical implementation, non-toxicity and cost-effectiveness are crucial factors. Fulfilling these prerequisites guarantees peak efficiency and durability [60].

4.2. Na-ion solid polymer electrolyte

SEs have been developed to reduce the hazards of LE combustion and leakage. These new electrolytes provide excellent ED and safety [60–62]. This approach presents a novel solution to address all these problems. The ideal SE for NIBs is a GPE due to its high ionic conductivity and good chemical and thermal stability [63]. Its CV curve, reversibility, and cyclic stability are all equivalent to those of LEs. When tested at room temperature, enhanced conductivity and lower activation energy are characteristics of most SEs. These features can mitigate the challenge of transforming chemical energy into electrical energy.

On the other hand, studies investigating the potential of SEs containing Na^+ for use in batteries are limited. The primary challenge of ion transport in SEs is the leading cause. Battery use in NIBs is limited because of their poor conductivity, which hinders the efficient transfer of Na^+, a necessary component in the battery's electrochemical processes [64–67].

4.3. The ionic electrolyte for NIBs

Fig. 4(a) shows the ionic electrolytes of NIB, a liquid containing all ions. ILs or greenhouse ions are materials with sufficiently long ions at or near room temperature [68,69]. In general, it consists of inorganic anions and organic cations. In addition to being non-volatile, the ionic LE offers a broad electrochemical spectrum [70,71]. IL monomers are transformed into polyconic liquids. One or both monomers—cations and anions—are incorporated into the polymer structure. Combining the best features of ILs with those of macromolecular molecules, polyconic liquids exhibit unique physical and chemical properties. Polyconic LEs, made by directly polymerizing IL monomers, provide a wide range of electrochemical stability, strong mechanical properties, and abundant lithium-ion pathways. Improved processability, permeation, and mechanical stability of polyconic liquids have made them attractive options for PEs [72]. The chemical transformation of some naturally occurring polymers by ILs may lead to the introduction of free anions or cations into their pore designs. This change improves the polymers' ionic conductivity in structure. This polyconic LE may maintain the remarkable mechanical characteristics of the primary polymer electrolyte. It is possible to get ideal conductivity by compounding the ILE, which has outstanding safety properties. However, the high cost of ILEs prevents their widespread use on a global scale [73].

4.4. Gel polymer electrolyte

In LIBs and NIBs, a GPE acts as an intermediate medium between the liquid and SEs. GPE offers a more thermally stable alternative to LEs while maintaining a similar level of ionic conductivity, theoretically ranging from 100 to 101 m Scm^{-1} [74,75]. This characteristic arises from the comparable compositions and conduction mechanism of both types of electrolytes. Moreover, GPE's unique design prevents the electrodes from coming into direct contact, reducing the risk of short circuits. Therefore, it replaces a battery separator while facilitating the conduction of ions like Li^+ and Na^+ [76]. However, these characteristics of GPE resemble SSEs without reaching similar mechanical strength or thermal runaway shielding [77–81].

The three main types of chemicals that make up GPE are ion-conducting salt (i), plasticizer (ii), and polymer (iii). To enhance the transport of Na^+ between electrodes, NIBs often use Na^+ conductive salts such as $NaPF_6$, NaTFSI, NaFSI, $NaCF_3SO_3$, $NaBF_4$, and $NaClO_4$ [82,83]. Each salt's specific qualities and limitations affect the performance and stability of batteries. The Na^+ source in GPE is the sodium salt, which produces Na^+ ions that enter through the gel matrix. With the addition of a plasticizer, GPE could accelerate diffusion and multiply the amount of mobile Na^+ ions. The polymer's glass transition temperature is also reduced since the plasticizer reduces its crystallinity. Ionic conductivity is, therefore, improved in the plasticized polymer electrolyte, even when exposed to typical environmental conditions [84].

The GPE with a precisely controlled structure shows outstanding stability in NIBs across various levels of current and long cycling periods given in Fig. 3(a). This is attributed to its efficient inner pore architecture and better compatibility with the electrodes. NIBs typically use

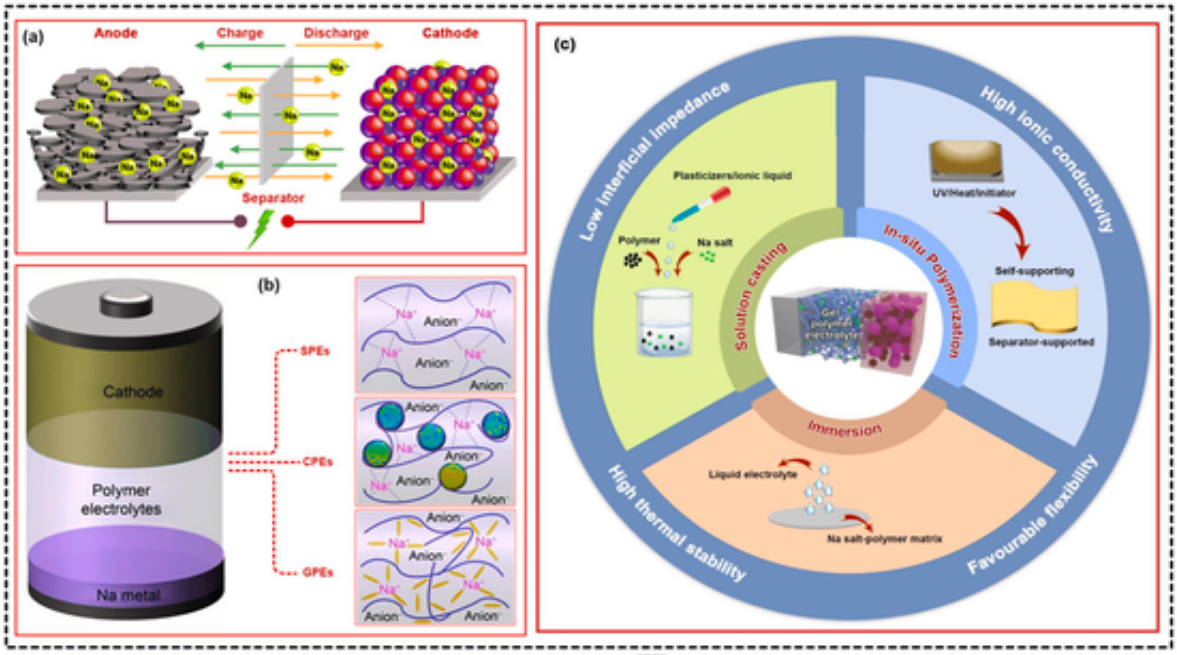

Fig. 4. **(a)** Schematic diagram of ion electrolyte in Na-ion battery **(b)** Schematic diagram of gel polymer electrolyte in Na-ion battery [114]. **(c)** Synthesis methods for the GPEs.

organic LEs together with a separator placed between the electrodes. Despite their poor thermal stability, porous polymer-based separators are the most suitable for LIBs. However, due to their distinct atomic characteristics, they are unsuitable for NIBs. Because of this, glass fiber (GF), although its thickness deviates significantly from the requirement, is frequently used as a separator for NIBs [85,86].

Furthermore, the direct electrode connection of the GF could result in thermal runaway and explosion because of its very porous, loosely woven design. Furthermore, capacity degradation can occur because of inadequate pore size. Despite limiting the progress of NIBs, most research in this field focuses primarily on electrode materials, neglecting the limitations posed by non-optimized porous separators [87]. To address these shortcomings, more studies must be into other separators as substitutes for GF. However, research indicates that these alternatives exhibit slightly mediocre cell properties because of their lower ionic conductivity. So far, enhancing ion transport via electrochemically stable polymers is a common and straightforward approach to modifying GF [88–90].

A prime example of a coating material often used for GF is the PVdF-HFP copolymer. For solid-state LIBs, this material is ideal because it maintains high levels of thermal and electrochemical stability over the whole voltage range. In contrast to conventional polyolefin-based separators, PVDF-HFP is more attracted to the LEs due to the fluorine in its main chain. Moreover, PVDF-HFP-based membranes retain tiny pores even after phase separation, resulting in significant trapped LEs and improved ionic conductivity. Consequently, PVDF-HFP-based membranes have the potential to exhibit stable and enhanced cell performance. To improve Na^+ flow, it is critical to control the pores architecture of the PVDF-HFP coated GF [91–93].

Table 1 compares different electrolytes used in NIBs. It concludes that GPEs have many advantages compared to alternative electrolytes. These advantages include nonflammability, rendering them safer than aqueous electrolytes, high ionic conductivity, and stability at elevated temperatures. GPEs can establish favorable interfacial contact with the anode and cathode, enhancing battery performance [94–96].

4.5. The encapsulating polymers of GPEs

GPEs are typically produced by adding a specific amount of liquid electrolyte to the polymer host system. The characteristics of polymer frameworks significantly impact GPE performance. Most of the polymer hosts used in GPEs for SIBs are derived from LIB systems. Some commonly used polymer skeletons for GPEs include PAN, PVDF, polymethyl methacrylate (PMMA), PVDFHFP, and polyethylene oxide (PEO).

4.6. PEO-based GPEs

PEO is a readily available and non-toxic material that can produce solids and GPEs. The PEO-based SPEs and GPEs are extensively studied in LIBs due to their excellent solvating power for Li salts and remarkable compatibility with Li electrodes [97]. The migration of Li^+ ions in PEO, a semicrystalline polymer with both amorphous and crystalline complexes,s, is limited to the amorphous portion due to the local mobility of polymer segments. The equivalent cells can only operate at higher temperatures, typically between 60 and 80 °C. On the other hand, SPEs based on PEO have a relatively low ionic conductivity of 10^{-6}-10^{-8} S cm^{-1}, which is lower than the conductivity at room temperature [98]. Researchers have made significant efforts to enhance electrolyte ionic conductivity and reduce PEO crystallinity. Adding plasticizers or inorganic fillers can improve the ionic conductivity of a PEO system. Adding IL to the PEO matrix significantly improves flexible polymer electrolytes' thermal and mechanical characteristics while enhancing their ionic conductivity. R. K. Singh's research group significantly improved the PEO system by incorporating IL of BMIM-MS and sodium methylsulfate (NaMS). The polymer electrolyte membranes have excellent thermal stability and demonstrate a high ionic conductivity of approximately 1.05 × 1^{-4} S cm^{-1} at 30 °C with a 60 wt% IL loading [99]. The PE described in the study exhibits remarkable thermal stability, a sodium-ion transference number of 0.39, and an impressive ionic conductivity of 4.1 × 10^{-4} S cm^{-1} at 30 °C. The electrolyte was synthesized using sodium bis(trifluoromethylsulfonyl)imide (NaTFSI) as the salt and another IL, BMIMTFSI, as the plasticizer. The performance of

Table 1
Comparison of different electrolytes used in Na-ion batteries.

Electrolytes	Properties	Ionic conductivity (mS cm^{-1})	Voltage	Capacity (mAh/g)	Energy density (Wh kg^{-1})	Retention rate (%)	Coulombic efficiency (%)	References
$NaClO_4$/NaOTF aqueous electrolyte	High ionic conductivity, low cost	95.25	1.75 V	–	70	87.5		[53]
NaWiSE aqueous electrolyte	Low cost, good conductivity	50	2.5 V	31	31	99.2	99.7	[54]
Aqueous/nonaqueous hybrid electrolyte	High conductivity	25	2.8 V	65	45	–	99.8	[55]
NMO/NTPO@C aqueous electrolyte	High flexibility, ionic conductivity, and long life	–	1.6 V	46	30	90	100	[56]
$NaClO_4(H_2O)_2AN_{2.4}$ electrolyte	High ionic conductivity	36.2	3.0 V	52	51	79.3	99	[56]
$Na_2MnFe(CN)_6$//$NaTi_2(PO_4)_3$ aqueous electrolyte	High ionic conductivity and energy density	–	2.8 V	117	–	81	–	[57]
KMnHCF/NaMnHCF framework	High specific capacity and low cost	–	–	108		96	–	[58]
NaFSI aqueous electrolyte	Low cost, high conductivity	90	2.6 V	–	–	–	–	[59]
multi-component aqueous electrolyte (MCAE)	High ionic conductivity	13.85	2.8 V	68	61	86	100	[60]
$NaMnO_2$–$NaTi_2(PO_4)_3$ hybrid aqueous electrolyte	High ionic conductivity	–	0.5 V–1.8 V	37	30	75	100	[61]
UV-cured solid polymer electrolytes	High ionic conductivity	–	3.0–5.5 V	–	114.7	91	–	[62]
A quasi-solid polymer electrolyte	High-capacity retention and voltage	1.06	5.85 V	125	–	–	97	[63]
A poly(DOL)-based quasi-solid electrolyte	High ionic conductivity	3.31	4.4 V	98.5	–	93.6	96.75	[64]
PEO/PNaMTFS polymer electrolyte blend	High ionic conductivity	5.84–7.74	4 V	–	–	–	100	[65]
Anion-trapping 3D fiber network enhanced polymer electrolyte (ATFPE)	High ionic conductivity	1.10×10^{-1}	5.98 V	117.5	–	87.1	99.89	[66]
PEO:NaBr solid polymer electrolyte films	High ionic conductivity	1.01×10^{-2}	–	–	–	–	–	[67]
Solvated double-layer quasi-solid polymer electrolyte (SDL-QSPE)	High Na^+ ion conductivity	1.2	5 V	80.4	–	–	100	[68]
PEO-based solid polymer electrolytes	High ionic conductivity	4.3×10^{-4}	–	–	–	–	–	[69]
PVDF/g–C_3N_4-Based Composite Polymer Electrolytes	Good mechanical properties and ionic conductivity	1.76×10^{-2}	0.1 V	100.3	–	81	99.5	[70]
Cross-linked solvent-free polymer electrolyte	Good mechanical properties and ionic conductivity	>1	0.01 V	–	–	–	–	[71]
Pyr14TFSI-NaTFSI ionic liquid-electrolyte	Thermal stability	10-100	2.7 V	100	–	99	–	[72]
NASICON Solid Electrolyte	high ionic conductivity	7.7×10^{-1}	0.5 V	84	–	95	>99	[73]
$Na_2Ti_3O_7$@C/Na half-cell with $NaCF_3SO_3$-based electrolyte	Improves the interfacial transport performance and highly conductive	–	0.01–2.5 V	98–177	–	–	76.5	[74]
Av ionogel electrolyte	High energy density and conductivity	0.9	4 V	–	400	–	99	[75]
asymmetric flame-retardant gel polymer electrolyte (A-FRGPE)	High cycling stability and ionic conductivity	2	5.63 V	114.9	–	96.1	99.99	[76]
Gel polymer composite electrolyte of beta-Al_2O_3 and PVDF-HFP	Good ionic conductivity	1.37	4.52 V	76.3	–	92.2	99.9	[77]
Boron-containing GPE (B-GPE)	Excellent mechanical properties	0.60	5 V	89–121	–	99.4	99	[78]
GPE system based on PCL	High Na^+-conductivity and suitable Na-storage propertie	1.3	4.3 V	–	–	–	–	[79]
Fluoroethylene carbonate (FEC) modified GPEs	High discharge capacity and ultra-long cycling stability	3.77	4.6	70–104	–	95.31	–	[80]
NWPH-GPE	High thermal and electrochemical stability	1.38	0.025 V	100.7	–	125	99.7	[81]
Polyisoprene-Based Single-Ion Gel Polymer Electrolyte	Air-stable, safe, cost-effective	1.81×10^{-2}	2.6–4 V	45–57	–	82	≥98	[82]
Gel polymer electrolyte with solvent adiponitrile and ethylene carbonate	Good ionic conductivity	4.6	5 V	85.47	–	–	71	[83]
gel polymer electrolytes with binary polymer matrix and binary plasticizer	Good ionic conductivity	15.5	5.2 V	18	–	70	–	[84]
Muscovite in gel polymer electrolyte	Excellent thermal stability	5.5	0.2 V	200	–	99	–	[85]

the $Na_{0.7}CoO_2$ cell was outstanding, both in terms of cycle performance and coulombic efficiency.

4.7. PVDF and PVDF-HFP-based GPEs

PVDF exhibits exceptional film characteristics and a high dielectric constant ($\varepsilon = 8.4$). This property enhances the solubility of salts within the polymer matrix, attributable to its repeating structural units of –CH_2-CF_2-.PVDF exhibits exceptional chemical and electrochemical stability, which can be attributed to three key factors. Firstly, it possesses a remarkably high glass transition temperature. Secondly, it contains a potent electron-withdrawing group of -C-F-. Lastly, it also boasts a high glass transition temperature. The PVDF-based polymer membranes can be quickly produced through solution casting or electrospinning, readily dissolving in common organic solvents. Janakiraman's team [100] significantly improved GPE performance by utilizing electrospinning techniques with various salts and solvents incorporated into PVDF. The PVDF GEs for NIBs were created by immersing the porous membrane in a LE at room temperature. The electrolyte options included either 1 M $NaClO_4$ in EC/DEC (1:1 vol%) or 1 M $NaPF_6$ in EC/PC (1.1 vol%). However, PVDF, a semicrystalline polymer, exhibits lower absorption of LEs. Introducing the HFP segment into PVDF chains can disrupt the reg-

ular segment structure and decrease crystallinity. These enhancements result in improved liquid holdup and increased ionic conductivity. The study conducted by Wu et al. utilized a 1 M $NaClO_4$-based carbonate solution (EC:DEC: DMC = 1:1:1, by volume) as a plasticizer. They focused on using PVDF-HFP as the polymer framework and achieved a satisfactory ionic conductivity of 6.0×10^{-4} S cm^{-1} at room temperature [101]. The Researchers D.T. et al. examined PVDF-HFP-based GEs that contained different LEs within the polymer matrix [102]. Porous PVdF-HFP membranes were generated using a phase separation approach. The samples were subsequently filled with either 1.0 M $NaClO_4$ or $NaPF_6$ in carbonates of PC and fluoroethylene carbonate (FEC) carbonates or 0.5 M NaTFSI in EMITFSI IL.

4.8. PMMA-based GPEs

The presence of neighboring methyl groups prevents polymethyl methacrylate from forming a regular and tight crystal structure, as it cannot spin around the C–C bond. This characteristic makes it an example of an amorphous polymer [103]. Furthermore, PMMA's ester groups react highly with LES, especially carbonate electrolytes. The enhanced ionic conductivity can be attributed to the polymer hosts' capacity to retain a more significant number of LEs effectively. However, PMMA does have a low mechanical strength. In most cases, the mechanical properties of GPEs are compromised to achieve improved ionic conductivity when PMMA is used. The mechanical stability and electrochemical performance of GPEs based on PMMA have been improved through various methods. These include incorporating nanofillers, blending with other polymers, and in situ crosslinking copolymerization. The GE developed by Kumar et al. demonstrated the ability to conduct Na^+ ions and was composed of PMMA, SiO_2, $NaClO_4$, and EC: PC [104]. The researchers found that the presence of SiO_2 nanofillers impacted the overall charge carrier mobility and their integration into GPE systems. Improving the mechanical properties of GPEs can be achieved through cross-linking, which is equally effective as incorporating inorganic fillers. Crosslinked polymer matrices can enhance the mechanical strength, LE retention rate, and plasticizer compatibility. The lab of Goodenough successfully developed an affordable GPE by utilizing in situ radical polymerization to create crosslinks in PMMA [105]. The composite GPEs demonstrate exceptional electrical properties, boasting a room temperature ionic conductivity of 6.2×10^{-3} S cm^{-1} and an impressive electrochemical window of 4.8 V (Vs. Na/Na^+). Compared to the conventional LE, this GPE exhibits the potential for enhancing the mechanical and interfacial properties of NIBs, especially at the evaluated temperature. The whole cell of $Na_3V_2(PO_4)_3$‖GPEs‖Sb demonstrates remarkable cycling stability, with a coulombic efficiency near 100 %.

4.9. PAN-based GPEs

PAN-based GPEs stand out from other PEs due to their antioxidative properties, high thermal stabilities, and ionic conductivity. Jyothi et al. [106] successfully produced a PAN-based GPE using a straightforward solution-casting method, using the plasticizing EC and dimethylformamide solvents. The presence of 30 wt% NaI at 30 °C results in an ionic conductivity of up to 2.35×10^{-4} S cm^{-1}, which is observed to vary with the concentration of NaI salt. In addition, electrolyte systems were developed using PAN/$NaClO_4$/EC/PC and PAN/Al_2O_3/NaF/EC. These systems exhibited ionic conductivities of 4.5×10^{-3} S cm^{-1} and 4.82×10^{-3} S cm^{-1}, respectively, at ambient temperature. Ahn et al. [107] conducted a study on the electrochemical performance of a battery system. They utilized a GPE of electrospun PAN nanofibrous membranes and a cathode material of a polyimide (PI)/multi-walled CNT nanocomposite. The NIB boasts an impressive lifespan of 3000 cycles and exhibits remarkable cycling stability at high C-rates. This is achieved by combining a GPE anode with an organic PI nanocomposite cathode. PAN-based GPEs can also be utilized in aqueous NIBs. Despite their subpar mechanical characteristics, using PAN-based GPEs in NIBs is restricted.

4.10. PVP-based PEs

Polyvinylpyrrolidone possesses abundant amide groups, significantly improving its biocompatibility and film-forming capabilities. This polymer could separate Na-ions and dissolve sodium salts. Chandrasekaran et al. [108] created a GPE using PEG, PC, and DMF as an example. The ideal ionic conductivity (6.71×10^{-5} S cm^{-1} at 35 °C) of the PVP/PEG/$NaClO_3$ electrolyte was achieved by incorporating 10 wt % PEG. Furthermore, Raja et al. and Chen et al. [109] developed PVP-based APEs using different sodium salts. The ionic conductivities of both APEs were found to be around 10^{-6} S cm^{-1} at room temperature. Further research could explore the potential of combining PVP with inorganic electrolytes or polymers known for their high ionic conductivities. Another avenue to explore is the creation of copolymers of N-vinylpyrrolidone and monomers that contain ion-conducting segments to address the issue of PVP-based PEs.

4.11. Thermal stability of GPEs

Thermal stability is crucial for ensuring the safety of GPEs. The battery's ability to endure high temperatures without encountering safety concerns such as short circuits or internal thermal runaway, which can occur when the electrolyte membrane deforms, relies on its thermal stability. The electrolyte should maintain its stability across the battery's operating temperature range. The expected temperature range for NIBs is −40 to 150 °C. The plasticizer and the polymer host frameworks influence the thermal stability of GPE. The thermal stabilities of nonaqueous LEs, such as carbonate esters and ethers, are relatively weak due to their low flash and boiling points. EC, PC, and FEC are notable for their higher flash points, making them more thermally stable. The usual LEs in this scenario are highly flammable and extremely volatile. However, the nonvolatility, nonflammability, and minimal vapor pressure at ambient temperature of ILs contribute to their impressive thermal stability. Triethyl phosphate (TEP) and other phosphonates are plasticizers that exhibit exceptional flame retardancy and thermal stability [115].

4.12. Mechanical stability of GPEs

The mechanical characteristics of GPEs significantly impact battery performance and cycle life. On the other hand, the formation of sodium dendrites can lead to a local short circuit in a battery. However, the membrane's exceptional mechanical strength can help prevent their formation. On the other hand, electrolytes with mechanical solid properties could support a variety of electrode materials, making them highly beneficial for flexible batteries. From research to mass manufacturing, that is a crucial element for batteries. Several factors complement each other when describing the mechanical characteristics of GPEs. Materials are often characterized using both the modulus of elasticity and the tensile strength. The classification of elastic modulus is based on the forces that act upon it, resulting in subdivisions such as Young's modulus, shear modulus, and bulk modulus. Two commonly used criteria for evaluating the mechanical properties of GPE are its tensile strength and Young's modulus. The tensile strength of an electrolyte material refers to the maximum tensile stress it can withstand before fracturing. Young's modulus demonstrates the material's resistance to elastic deformation, which quantifies the relationship between the material's tensile stress and strain during deformation. Y. Chen et al. [110] developed and manufactured a composite GPE consisting of graphene oxide (GO) and PVDF-HFP. The compressive strength of composite GPE's Young's modulus of 2.5 G Pa effectively prevents the for-

mation of sodium dendrites, achieved by incorporating 2 wt% GO content, resulting in a significant tenfold increase.

4.13. Interfacial stability of GPEs

It is of utmost important to maintain the stability of the electrolyte-electrode interface when designing NIBs for practical applications. The electrolyte should not react with the electrode while the battery is on standby, an essential requirement. Furthermore, the electrolyte and negative electrode must form a thick and uniform SE interface film during charging and discharging to ensure a reliable plating and stripping process for sodium ions. This step is crucial to avoid several potential hazards. By neglecting this step, the battery's capacity can be significantly reduced due to the formation of sodium dendrites, also known as "dead sodium."

Additionally, there is an increased risk of internal short circuits, thermal runaway, and even explosions if the dendrites penetrate the electrolyte/separator and reach the positive electrodes. The interface difficulties and SEI in batteries, such as LIBs and SIBs, have been extensively studied due to their crucial role and the challenges involved in understanding them. The stability of battery cycles is highly dependent on the quality of the SEI film, which needs to be dense and uniform. However, this film protects against side reactions and increases interface resistance. Considerable effort is being dedicated to developing more effective methods for producing SEI material that exhibits stability and corrosion resistance. The SEI film in the NaF component is enhanced by adding additives like fluoroethylene carbonate to the electrolyte [111]. The homogeneous deposition of sodium ions on the anode is encouraged by this. The compatibility of GPEs made via in situ polymerization surpasses SEs in sodium anodes. In situ polymerization is another method to enhance electrolyte-electrode compatibility at the interface.

5. Synthesis techniques for GPEs

Here, we will discuss in detail the different strategies and techniques that are being utilized for the synthesis of GPEs. The strategy for the GPEs is simple. Preparing GPEs involves blending a salt with an organic liquid plasticizing solvent and subsequently incorporating the mixture into a polymer to establish mechanical stability [112]. This can be attained by different synthesizing techniques, like the immersion approach, solution casting approach, and in-situ polymerization route [113]. The details and analysis of the different techniques are discussed along with the comparison in Table 2.

5.1. Immersion approach

The immersion technique represents a straightforward technique to produce GPEs, involving the swelling of dry polymer membranes in organic LEs. This method carefully chooses an appropriate polymer substrate, and polymer membranes of varying sizes, thicknesses, and porosities are generated through the solution, phase separation, or electrospinning techniques [114,116]. Li et al. fabricated PVDF/PEO nanofibrous membranes using the electrospinning technique, as illustrated in Fig. 4(c). Initially, PVDF and PEO, dried beforehand, are dissolved in DMF at a specific weight ratio and subjected to mechanical stirring for 24 h at room temperature. The polymer concentration blend solution is set at 0.15 g/ml. Following a 1-h standing period to eliminate air bubbles, the viscous polymer solution is introduced into the needle injection pump. The needle's tip, connected to a high-voltage source, undergoes electrospinning under ambient conditions. The process is straightforward and does not require sophisticated equipment, making it cost-effective. It ensures uniform electrolyte distribution and can be applied to various polymers and electrolytes. However, this method has some limitations. Like, the complete removal of solvent can be challenging; hence, residual solvent can negatively affect the performance of GPE.

Table 2
Comparison between different synthesis techniques for GPE.

Immersion techniques	Solution casting approach	In situ polymerization approach
Principal		
• Involves immersing a pre-formed polymer membrane into an electrolyte solution to impregnate it with liquid electrolyte	• Polymer and electrolyte are dissolved in a common solvent followed by casting the solution into a desired shape and evaporating the solvent to form a gel polymer electrolyte	• Polymerization of monomers and simultaneous incorporation of electrolyte components to form the gel electrolyte within the desired structure
Advantages		
• Simplicity and ease of the process. • Well-suited for thin and flexible polymer membranes. • Minimal equipment requirements.	• Precise control over the composition and homogeneity. • Ability to tailor the electrolyte and polymer matrix. • Enhanced interfacial contact between polymer and electrolyte	• Excellent control over the polymer structure and electrolyte content. • Enhanced compatibility between polymer and electrolyte phases. • Potential for tailoring properties by adjusting polymerization conditions.
Drawbacks		
• Limited control over the electrolyte distribution within the polymer matrix. • Difficulty in achieving a uniform electrolyte content. • Potential for poor adhesion between the polymer and electrolyte phases	• Requires careful solvent selection to prevent adverse effects on polymer structure. • Potential challenges in removing residual solvent completely. • Limited scalability for large-scale production	• Complexity in handling reactive monomers and initiating polymerization. • Equipment and reaction conditions need careful optimization. • Batch-to-batch variability in polymerization kinetics

5.2. Solution approach

In the solution approach, membranes are soaked in the desired organic electrolyte, swelling and expelling excess liquid. The outcome is a flexible GE membrane with high ionic conductivity [117]. To enhance mechanical strength and thermal stability, inorganic fillers can be introduced during the preparation of the polymer membranes [118,119]. This method is usually considered for the large-scale production of GE membranes. The electrochemical performance of the polymer precursor membrane hinges on its properties and highlights the critical importance of the polymer membrane preparation method. Presently, widely utilized synthesis approaches incorporate solutions in phase separation. This approach offers the polymer in an organic solvent and applies the film through the casting technique. In contrast to phase separation, this technique is characterized by its simplicity, cost-effectiveness, and controllability. The resulting electrolyte membranes demonstrate a high degree of consistency in their properties. Conversely, phase separation can induce pore formation, a desirable trait for facilitating electrolyte adsorption and achieving high ionic conductivity. The solution synthesis method holds promise for large-scale applications [120–122]. Su et al. prepared a GPE for Na-ion conduction, employing PVDF-HFP. PVDF-HFP membrane immersed in an electrolyte of 1 mol/L $NaClO_4$ with flu-

orinated EC and PC solvents, serving the dual role of electrolyte and separator [123].

In NIBs employing polymer, the improvement of ionic conductivity is directly achieved by incorporating ceramic fillers. This is attributed to the following reasons: The addition of ceramic fillers deployed the crystallinity of polymers, facilitating structural alteration of Na^+ conducting pathways and the polymer chains on the filler surface. The creation of an "*ionic ceramic complex*" occurs according to Lewis acid-base interaction, facilitating sodium salt dissociation. Furthermore, this consistent dispersion of inorganic fillers as a rigid framework improves its mechanical strength and dissipates heat. This, in turn, alleviates thermal degradation of electrode materials.

Additionally, fillers positively impact interface stability by enhancing interactions among the surface functional groups and the electrode material. Moreover, fillers can contribute to the stable interfacial layer, leading to severe improvements in the cyclic capability of NIBs [124–128]. This method's key features include homogeneous composition with fine thickness control. However, for this technique, the choice of solvent is difficult, dissolving both polymer and electrolyte salt, thus limiting the range of materials that can be employed.

5.3. Solution casting approach

In this technique, polymer, plasticizer, sodium salt, and filler are collectively heated and stirred for homogeneous dissolution of components. This mixture is then cast and dried, resulting in GPE. The choice of plasticizers is made from solvents like EC, DEC, PC, FEC, and ether, or they may be ILs with a high and sharp melting point and nonflammability. Compared to the immersion technique, the gel membrane synthesized through the solution casting technique exhibits more vital intermolecular interaction. Specifically, the plasticizers get bonded to the polymer chain by nucleophilic substitution, dehalogenation, and other reactions during mixing, resulting in enhanced thermal stability of the resulting GPE membrane [129–137]. Careful selection of the plasticizer and polymer is essential to achieve a harmonious balance among high ionic conductivity, interfacial contact, thermal stability, and mechanical strength through their interaction. For instance, Chen and his colleagues employed a solution casting technique to fabricate a highly conductive GPE consisting of PVC (7.5 %), PVDF (17.5 %), $NaClO_4$ (8 %), and PC (67 %). Results demonstrated the incorporation of PVC, resulting in poor crystallinity and facilitating rapid movement of Na^+ ions within the polymer network, limiting its broad range applicability [138]. Singh et al. utilized the solution casting method to describe a GPE containing sodium bis(trifluoromethyl sulfonyl)imide NaTFSI, polyethylene oxide (PEO), and ionic I-butyl-3-methylimidazolium bis (trifluoromethyl sulfonyl)imide (BMIMTFSI) liquid (10–40 %), serving as plasticizer [139]. This technique provides high ionic conductivity and allows the incorporation of various polymers, salts, and additives, thus enabling customization of the electrolytes' properties to suit specific applications. However, this method is time-consuming, and phase separation is risky during solvent evaporation.

5.4. In situ polymerization approach

In-situ polymerization refers to the polymerization of tiny monomers or solvent molecules under controllable conditions involving heat, light, or the presence of an initiator. This method effectively achieves stable interfaces even at the mass production level. Compared to the other approaches, the in-situ polymerization of GPE involves the crosslinking of long and short chains, forming an amorphous network architecture that boasts remarkable ionic conductivity and mechanical strength. Within this crosslinked network, unpolymerized small molecules become confined through bonding, contributing to improved safety and thermal stability of the GPE. Additionally, during the polymerization process, an interfacial layer is directly created on the electrode surfaces, reducing the catalytic decomposition of the GPE due to cathode bodies and the simultaneous creation of sodium dendrites. This dual function enhances interface contact significantly, showing greater homogeneity, leading to an overall improvement in performance [140–144].

Employing in-situ polymerization of electrolytes over supported membranes proves to be an effective method for producing GPEs, characterized by high ionic conductivity, favorable interfacial contacts, and superior mechanical strength and stability. Essential criteria for a self-supporting membrane encompass uniform thickness, low interface resistance, appropriate porosity facilitating ion penetration while preventing cathode-anode contact, adequate mechanical strength to avert fracture and short circuits, and thermal and chemical stability crucial for suppressing side reactions and ensuring safety. While current polypropylene separators meet these requirements, advancements in self-supporting membranes through surface functional design are imperative for achieving heightened battery energy density. To illustrate, precise control of membrane thickness and electrolyte ratios is vital to prevent a substantial reduction in energy density [145–148]. Table 3 shows different types of GPE along with their ionic conductivity and Na^+ ion transference rate [149–156]. This technique provides excellent interfacial adhesion and uniform properties, and it is highly customizable due to the inclusion of various monomers, cross-linkers, and additives. As in this, more ingredients are involved, making the process complex.

In summary, the immersion approach for GPE preparation involves swelling dry polymer membranes in organic LEs, utilizing various methods to create membranes of multiple sizes and porosity. These membranes were then soaked in the organic electrolyte to achieve a flexible GE membrane with higher ionic conductivity, with the option to include inorganic fillers for enhanced mechanical strength and thermal stability. This method shows promise for large-scale fabrication. In comparison, the solution casting technique combines polymer, sodium salt, plasticizer, and a filler, forming GPE with stronger intermolecular

Table 3
Overview of different types of GPE and their ionic conductivity.

Process	Type of GPEs	Ionic conductivity (m Scm^{-1})	Na^+ ion transport number	References
Phase separation	Poly(vinylidene difluoride-co-hexafluoropropylene)	0.60	–	[38]
solution casting	solution of $NaCF_3SO_3$ (sodium triflate or NaTf) in a room temperature ionic liquid 1-ethyl 3-methyl imidazolium trifluoro-methane sulfonate (EMI-triflate or EMITf) immobilized in poly (vinylidine fluoride-co-hexafluoropropylene) (PVdF-HFP)	5.74	~ 0.23	[39]
Immersion	Polyvinylidene fluoride – hexafluoropropylene (PVdF – HFP)	1–2	–	[40]
	Poly-acrylonitrile (PAN)-based gel-polymer electrolytes formed with $NaClO_4$	4.5	–	[41]
Solution casting	trifluoromethane sulfonate (Na-triflate or NaTf)	6.3–6.8	~0.27	[42]
	Polyacrylonitrile-based gel-polymer	1.8	0.85–0.89	[43]
	sodium conductive $Na_3Zr_2Si_2PO_{12}$ nanoparticles modified PVDF-HFP/PMMA/TPU-based GPEs are prepared	2.83		[44]
	Poly(vinylidene fluoride-co-hexafluoropropylene)/poly (methyl methacrylate)	2.39	0.48	[45]

interactions and better thermal stability by the plasticizer bonding to the polymer chain. On the other hand, in situ polymerization, achieved under conditions like light, heat, or initiator presence, offers stable interfaces and mass production advantages, distinguishing itself from immersion and solution casting methods.

6. Preparation of electrodes for NIB

Based on Robert and co-workers' work, the study describes a method for creating electrodes. The cathode slurry was prepared through a combination of carbon-coated NaNMST ($NaNi_{1/2}Mn_{1/4}Sn_{1/8}Ti_{1/8}O_2$) acts as a primary active material with conductive carbon black to enhance the conductivity within the composite electrode. 8 wt% PVDF binder was used to ensure mechanical cohesion b/w active material particles. These compounds were assorted in a mass ratio of 89:6:5 (NaNMST: carbon black: PVDF) using NMP solution as a solvent. The Thinky ARE-250 planetary mixer was used to treat the cathode ink inside a sealed plot [157]. The mixing occurred within a mounters dry room maintained below a 40 °C due point to minimize moisture exposure. Material pre-measurement occurred under a recirculating fume hood in a dry room or an argon-filled glovebox to ensure minimal moisture exposure. The mixing process employed a three-step sequence: critical dispersion, conductive additive incorporation, and binder addition. The prepared cathode slurry was doctor-bladed onto aluminum current collector substrates. The blade gap was set to 150, targeting an 80 g/m^2 final electrode loading. To achieve quick solvent evaporation, the electrodes were dried for 40 min at 80 °C on a hot plate. After that, moisture from these electrodes was dried using a vacuum oven chamber at 120 °C [158]. The complete manufacturing method is demonstrated in Fig. 5.

The cathode slurry was found to have 70 wt% of the electrochemically active $NaTi_2$ $(PO_4)_3$, 20 wt% of it consists of conductive carbon black (super-P, TIMCAL), and only 10 wt% of PVDF binder (HSV1800, Kynar) according to an ALD investigation on conformal electrode coatings for aqueous NIB electrodes. NMP (Sigma Aldrich) 99.5 % served as processing solvent. The slurry underwent planetary ball milling at 900 rpm for 1 h to achieve a homogenous mixture. Subsequently, the slurry was thinned out using a doctoral blade and vacuum-dehydrated for 3 h at 120 °C. These films were then transferred and pressed into 316L stainless steel mesh current collectors with an approximate diameter of 1.3 cm^2. Each electrode had an average loading of 2.0 ± 3 mg of active material. The electrodes were further modified with a thin film coating using ALD in the exposure anode. This technique allows for the deposition of highly structured surface layers on electrodes, potentially influencing their electrochemical performance. Al_2O_3, TiO_2, and HfO_2 were employed as coating materials at a reactor temperature of 170 °C [159].

A cathode slurry was formulated by combining 94 wt% $Na_3V_2(PO_4)_3$/C composite (comprising 93 wt% $Na_3V_2(PO_4)_3$ and 7 wt% carbon) with 3 % of weighted percentages of conductive carbon black and PVDF as binder. The NMP-based solvent was employed for effective dispersion using a dissolver mixer. Using a knife coating technique, the synthesized cathode slurry was then coated upon the 20 μm aluminum current collector. Subsequently, the coated current collector dried at sequential temperatures of 80 °C and 120 °C to remove residual solvent. Finally, calendaring was applied to the dried cathode electrode to achieve a flat and dense morphology. The anode slurry was prepared by combining 93 wt% commercially sourced coconut shell-derived HC with 1 wt% conductive carbon black to enhance electrical conductivity within the electrode. A dual binder system contains 1.87 wt% of carboxymethyl cellulose (CMC) and 3.73 wt% of styrene-butadiene rubber (SBR). This combination likely facilitates strong adhesion between HC particles CMC while offering additional mechanical stability and flexibility during cycling SBR. Water was chosen as the solvent due to its compatibility with CMC [160].

6.1. Coin cell preparation and assembly

The overall steps for creating a coin cell and assembling it for an NIB are similar to those for a LIB, with the main difference being using sodium metal instead. The authors described a method for coin cell fabrication utilizing $LiCoO_2$ as the active cathode material. An 80 wt % $LiCoO_2$, 10 wt % carbon (black), and 10 wt % PVDF (binder mixture) in NMP was prepared as the electrode slurry for LIBs. After that, this slurry was doctor-bladed onto aluminum current collectors and copper for preferred cathode and anode materials. To ensure total moisture re-

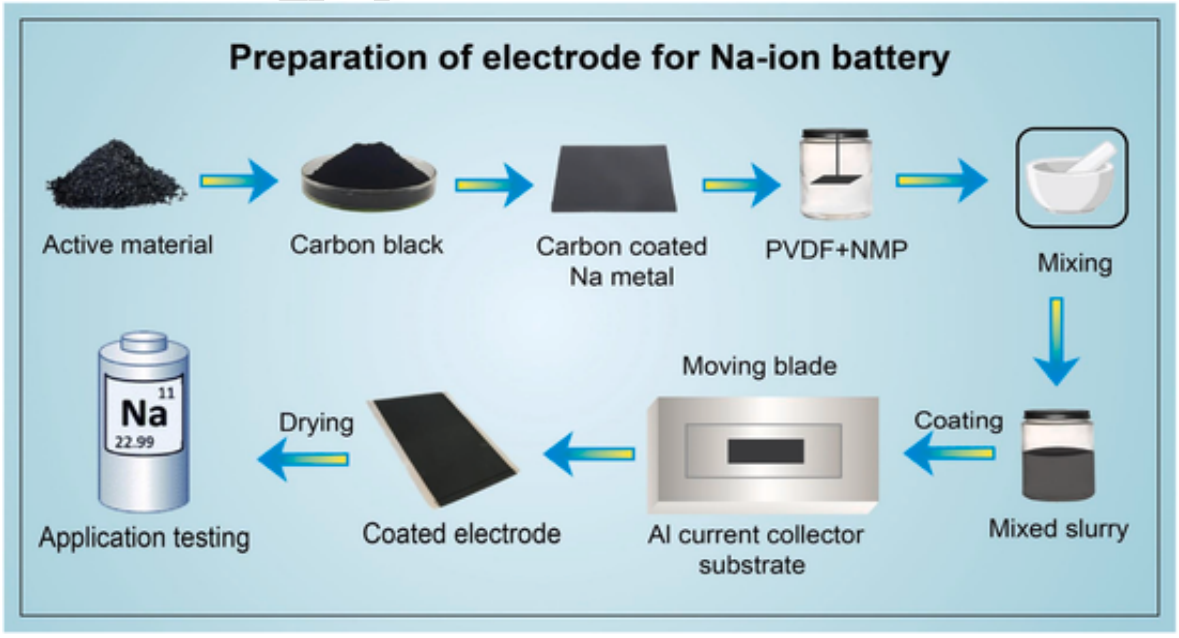

Fig. 5. The synthesis diagram for the fabrication of electrodes for the NIB.

moval, these coated electrodes were dried (either in the air or under volume) at 90–120 °C for 2–8 h, as seen in Fig. 6(b).

Lithium foil served as the counter electrode in the cell assembly, which used a 1M $LiPF_6$ electrolyte solution in a carbonate solvent mixture (ECD: MC: DEC). The entire coin cell assembly was carried out inside a glove box filled with argon to reduce unwanted reactions. Celgard C480 microporous membranes (19 mm diameter) were taken as separators to prepare the coin cell. All cell components, including coin cell cases, spacers, springs, separators, and working electrodes, were transferred into a glove box for assembly under an inert argon atmosphere. A controlled amount of electrolyte solution (1M $LiPF_6$ in EC: DMC: DEC) was dispensed onto the cell cup, followed by the placement of the working electrode. This sequence was repeated by adding two separators, each separated by a controlled amount of electrolyte. Lastly, a spring, two stainless steel spacers, and the Na^+ counter electrode were inserted. The cell was then sealed using a crimping machine, ensuring a tight closure to prevent leakage. Plastic tweezers were employed throughout the assembly process to minimize the risk of short-circuiting. After cleaning any excess electrolytes with a wipe, the completed coin cells were removed from the glove box [161].

6.2. Preparation of coin cell for NIB

Fig. 6 (a) shows the preparation of a coin cell for an NIB. Sodium foil is employed as a counter electrode. Celgard 2400 was employed as a separator, while an electrolyte 1M solution of $NaPF_6$ in EC/DMC following a 1:1 ratio by volume was chosen. Following the above-mentioned method, these cells were prepared in a glove box filled with argon [162].

6.3. Tee union Swagelok cell configuration

Three electrodes on a Swagelok cell were employed for characterization. A slurry of 5 % carbon black, 90 % HC, and 5 % PVDF binder was used to fabricate the working electrode using a doctor blade technique on an aluminum current collector covered with carbon. Following a 90-min drying process at 120 °C in a sealed oven, the electrodes were integrated into the Swagelok cell.

This three-electrode setup differs from the standard two-electrode version by utilizing a Tee-Union design to accommodate a reference electrode alongside the counter and working electrodes. A typical Swagelok cell's counter, separator, and working electrode reside within the union's straight body. The three-electrode configuration positions the reference electrode and an additional separator perpendicular to the standard cell stack within the Tee-Union. The reference electrode itself is prepared by filling sodium metal into the acceptor attachment of the Tee-Union.

Two distinct separators were chosen to ensure low resistance and good cycling stability with the reference electrode. A Celgard 2500 polypropylene separator provided electrical insulation between the reference electrode and the cell stack, while a GF/A GF separator separated the counter and working electrodes. Finally, an electrolyte solution of $NaPF_6$ in a 1:1 vol ratio following EC: DEC permeated all electrodes and separators within the cell.

Because less current flows through the reference electrode in this three-electrode design, the counter and working electrodes can be monitored simultaneously while the device is operating [163].

7. Electrochemical properties of GPEs

GPEs have garnered much attention in energy conservation storage because of their unique electrochemical attributes. Previous research has highlighted their critical role in enhancing the efficiency and dependability of ESDs. An in-depth analysis of several GP composites highlights the importance of this parameter in maximizing the durability and efficiency of ESDs. Understanding their electrochemical behavior is critical to progressing the creation of next-generation ESDs.

Gao et al. prepared a cost-effective composite GP/GF electrolyte using PVDF-HFP reinforced by a GF paper. A polydopamine coating was added to improve the PVDF-HEP's mechanical and surface qualities and prepare it for use in a NIB [164]. The composite polymer matrix demonstrates outstanding thermal stability and mechanical strength, maintaining these properties up to 200 °C. After saturation with a LE, the composite GP/GF electrolyte achieves a broad electrochemical window and high ionic conductivity. In NIB tests employing $Na_2MnFe(CN)_6$ as the cathode, the composite electrolyte exhibits enhanced rate capability, cyclic performance, and coulombic efficiency (CE). At a current density of 0.2 C, the discharge capacity of $Na_2MnFe(CN)_6$ is approximately 131 and 129 $mAhg^{-1}$ for the GF separator and GF/PVDF-HFP (GPH) composite GPE, respectively. A little increase in discharge capacity was observed for the GF/PVDF-HFP/PDA (GPHP) membrane with 131.1 $mAhg^{-1}$ current density. The CE significantly improved from 86.0 % for the GF separator saturated with LEs to 98.1 % for GPH and 98.4 % for GPHP composite GPEs.

The incorporation of GF paper enhances the thermal stability of composite GPEs. Furthermore, it widens the electrochemical window, making it compatible with different electrode structures. The polydopamine coating further boosts the ionic conductivity of the GPEs, nearing that of LEs. Utilizing these GPEs significantly enhances the electrochemical properties of Na-ion half cells with $Na_2MnFe(CN)_6$ as potential cathodes.

Using a self-catalyzed approach, Niu et al. developed an innovative GPE with a crosslinked polyether network (GPE-CPN). In this method, the successful in-situ copolymerization of two monomers, trimethylol-

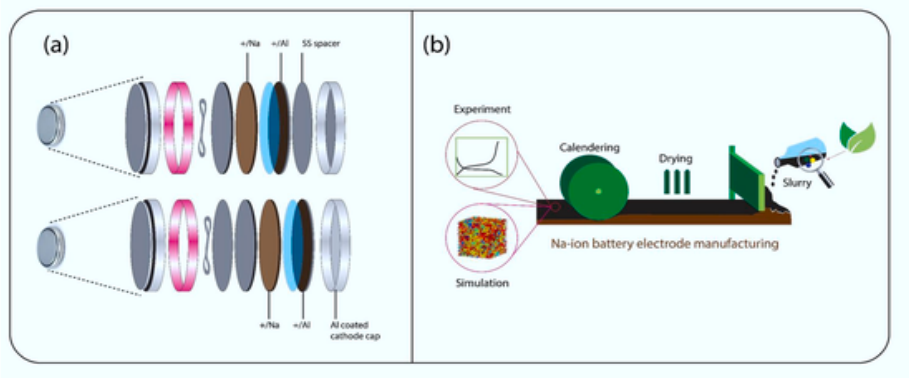

Fig. 6. (a) Procedure of crafting coin cell assembly **(b)** Fabrication process of electrode.

propane triglycidyl ether, and 1,3-dioxolane, was attained at a moderate temperature with the help of $NaPF_6$ as an initiator [165]. They have shown that the prepared GPE-CPN exhibits excellent electrochemical stability with a potential window of up to 4 V (vs Na^+/Na). It also demonstrates substantial ionic conductivity, measuring 8.2×10^{-4} S/cm at moderate room temperature. This high ionic conductivity is sufficient to inhibit the formation of sodium dendrites, thereby enhancing the stability of the sodium anode and electrolyte interface by analyzing the cross-sectional FESEM data of the composite membrane and surfaces of the cellulose. They were able to examine the progress of the in-situ polymerization process.

Additionally, they captured optical images illustrating the LE, which contains monomers and GPE-CPN, as shown in Fig. 7. The cellulose membrane consisted of interlaced fibers, leaving gaps of various sizes between them. The GPE filled the holes in the separator membrane after injecting the precursor electrolyte solution into it for 10 h. The cross-sectional view showed no apparent gaps, supporting the complete and successful gelation inside the membrane. Fig. 8(a) compares the electrochemical stability of the LE and GPE using LSV. The GPE showed a stable potential window up to 4 V, similar to the LE (1 M $NaPF_6$ in EC-DEC + 5 % FEC). Above 4 V, the liquid system started slowly breaking down, primarily due to solvents EC and FEC oxidizing. In contrast, the GPE maintained above 4 V. When subjected to an electrochemical cycle at a current density (0.5 mA/cm^2), it became evident that the GPE system displayed superior cyclic stability compared to the traditional LE system. In contrast, the LE system experienced enhanced polarization and eventually became short-circuited after 170 h. On the other hand, the GPE system maintained its deposition-stripping- properties after 400 h, as illustrated in Fig. 8 (b). Following the cycle test, the metallic Na surface in the LE system exhibited a rough and porous texture. Additionally, a significant sodium percentage of waste had detached and quickly adhered to the GF membrane, as shown in Fig. 7(e) and (f). Conversely, the metal Na surface, utilizing GPE, displayed a comparatively flat and smooth texture, as depicted in Fig. 7(g) and (h). Notably, there was no significant presence of dendrites, indicating that GPE effectively prevented the growth of sodium dendrites. LSV analysis indicated that both systems could deliver a C_{sp} of approximately 90 mAhg^{-1} at 10^{-1} C, as depicted in Fig. 8(c). To validate the versatility of the GPE, the electrochemical characteristics of other electrode materials, such as $Na(Li_{0.05}Ni_{0.3}Mn_{0.5}Cu_{0.1}Mg_{0.05})O_2$ and $NaTi_2(PO_4)_3$, were examined, as shown in Fig. 8(d). These materials retained high C_{sp} of 110 and 80 mAhg^{-1} at 10^{-1} C while demonstrating good stability. Niu et al. have devised a novel approach to fabricate crosslinked three-dimensional GPE cells utilizing a self-catalyzed in situ cationic polymerization that is sparkled by sodium salts. With electrode material, including metallic sodium, the GPE exhibits outstanding electrochemical performance, high ionic conductivity at room temperature, and excellent thermal stability. Consequently, the -rechargeable NIB utilizing this GPE exhibits superior interfacial stability compared to conventional LE systems.

A composite GPE with a crosslinked architecture made of beta-Al_2O_3 powders modified with silane and implanted in a PVDF-HFP matrix has been presented by Lai et al. This approach effectively eliminates the incompatibility issues at the inorganic-organic interfaces and significantly improves the electrochemical properties of the composite-based electrolyte. According to experimental findings, the resulting composite-based electrolyte has a remarkable sodium-ion transference number (t^+) of up to 0.424 and an enhanced Ionic conductivity of 1.37×10^{-3} S/cm at 20 °C [166]. The images in Fig. 9(a–c) illustrate the morphology of PSBX films with varying percentages of beta-Al_2O_3. These films exhibit relatively uniform surface pores, and when the powder reaches 60 wt%, beta-Al_2O_3 particles become visible on the film's surface. Fig. 9(d) shows that the PSB60 film has a thickness of around 300 μm. LSV is used to measure the electrochemical stability of PSBx-GPE. As depicted in Fig. 9(e), the data shows that the currents in PSBx-GPE stayed constant when the voltage was lower than 4.52 V. This observation highlights the higher voltage stability of PSBx-GPE.

In Fig. 9(f), a Na-ion transference number (t^+) of 0.424 is demonstrated for PSB60-GPE. This represents an enhancement in comparison to the transference number of P-GPE. To elucidate the alteration in the Na transfer pathway within PB60 and PSB60, 23Na NMR tests are conducted to evaluate the chemical environment of Na^+. To assess the interfacial stability of PSB60-GPE, P-GPE, and LE in the presence of a sodium electrode, symmetric cells are subjected to GCD at 0.5 mA cm^{-2}. As depicted in Fig. 10(a), the symmetric cell using PSB60-GPE shows remarkable stability for over 800 h, surpassing the stability of cells using P-GPE and LE. Moreover, the critical current density (CCD) of PSB60-GPE is evaluated in a symmetric cell. Fig. 9(g) illustrates that PSB60-GPE achieves a high CCD value of up to 2.2 mA cm^{-2}.

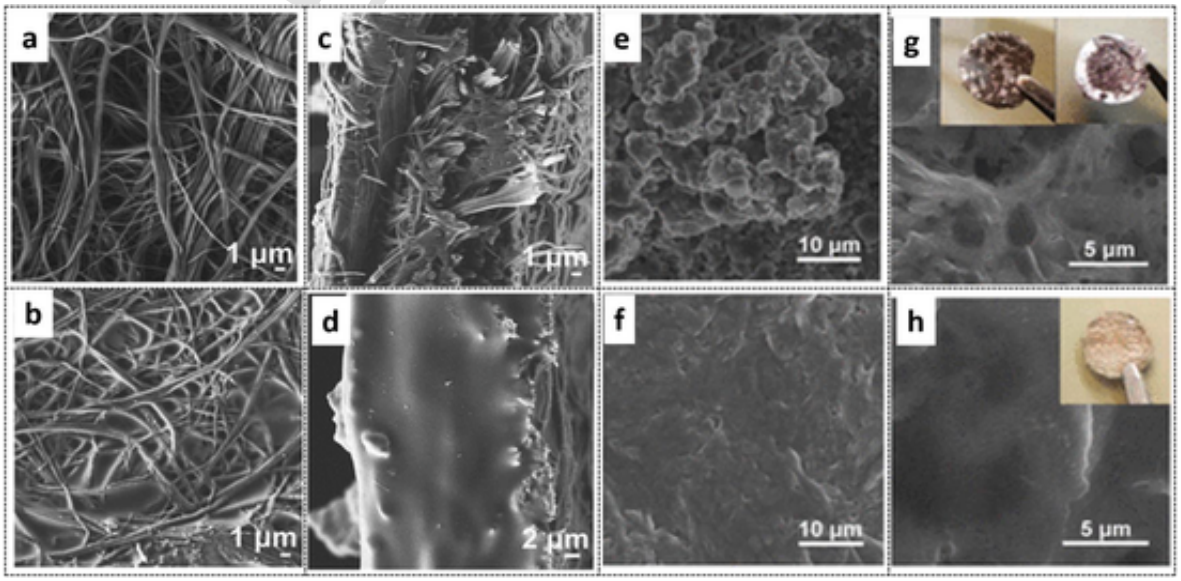

Fig. 7. FESEM images of **(a and b)** cellulose membrane and **(c and d)** gel composite membrane. FESEM images of the surface of the Na electrode in the **(e and f)** liquid and **(g and h)** gel system after galvanostatic cycling. (Insets are the corresponding optical images of the Na electrodes or separator after cycles.). With permission from Ref. [165] copyrights 2020, CCS chemistry.

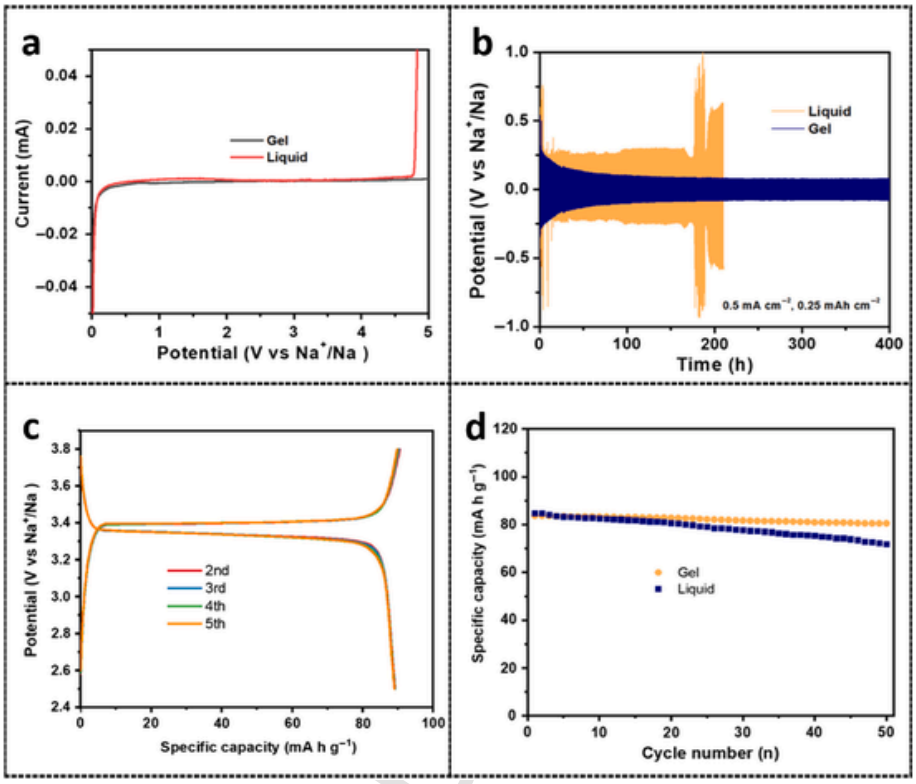

Fig. 8. **(a)** Analyzed electrochemical stability window of gel and liquid electrolyte by LSV **(b)** Analysis of Na deposition/stripping of Na-symmetric cells based on gel and liquid electrolytes at a current density of 0.5 mA cm^{-2} **(c)** Charge–discharge profiles based on liquid electrolyte at 0.1 C **(d)** Cycle performance of full-cells based on $Na_3V_2(PO_4)_3$ cathode and hard carbon anode with liquid and gel electrolyte at 0.1 C. With permission from Ref. [165] copyrights 2020, CCS chemistry.

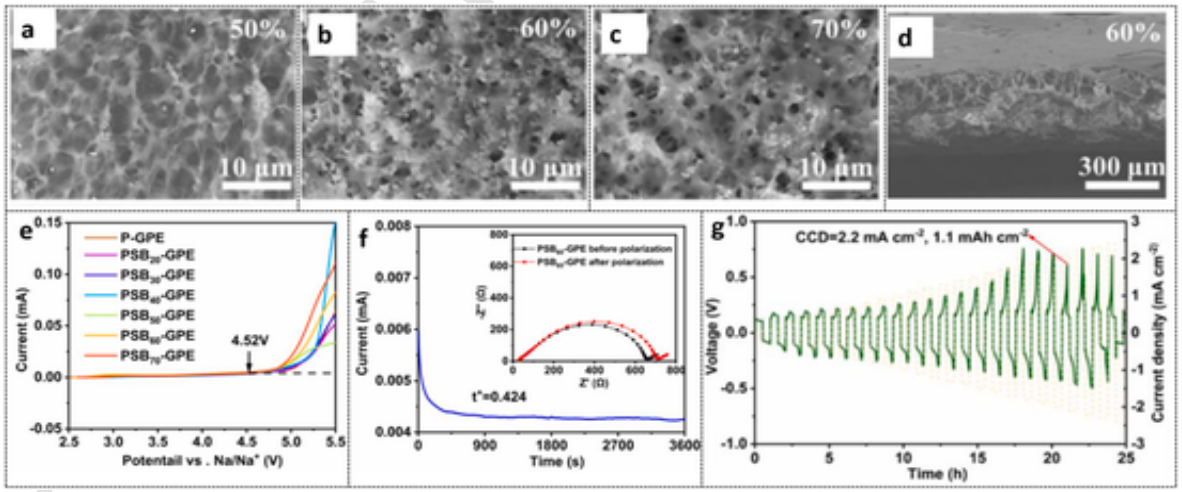

Fig. 9. SEM images for the surface of **(a)** PSB50, **(b)** PSB60, **(c)** PSB70 and **(d)** cross-section of PSB60 **(e)** LSV curves of PSBx-GPE operated from 2.5 V to 5.5 V at a scanning rate of 5 mV s^{-1} **(f)** Chronoamperometry curve of PSB60-GPE tested by a polarization of 5 mV, with the interfacial impedance before and after polarization inserted **(g)** CCD measurement of PSB60-GPE based symmetric cell (30 min per single cycle). With permission from Ref. [166] copyrights 2023, Energy Storage Materials.

In Fig. 10(a–d), SEM images depict the sodium electrodes after disassembly following 1000 cycles at 3 C. Notably, in the PSB60-GPE-based entire cell, the sodium surface remains relatively flat and smooth, with no apparent sodium dendrites. Furthermore, when operated at a rate of less than 3 C, the whole cell using PSB60-GPE exhibits minimal voltage polarization, as demonstrated in Fig. 10(e). Even at a high discharge rate of 5 C, the initial discharge C_{sp} remains as high as 86 mAh/g, and the retention is maintained at 89 % after 300 cycles, as illustrated in Fig. 10(f) furthermore, Fig. 10(g) shows that the PSB60-GPE-based symmetric cell exhibits good stability for more than 800 h, which is significantly better than that of P-GPE and LE-based symmetric cells.

In conclusion, a composite electrolyte comprising beta-Al_2O_3 and PVDF-HFP has been successfully synthesized using beta-Al_2O_3 powders as both the initializer and ionic conductive filler. This modification re-

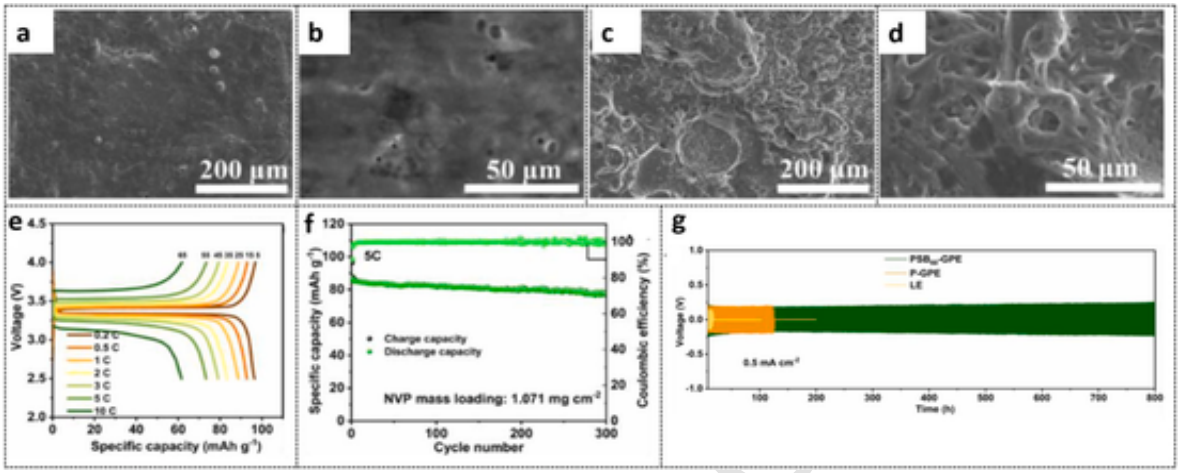

Fig. 10. (a) and (b) Sodium anode surface of PSB60-GPE based full cell after 1000 cycles at 3 C. **(c) and (d)** Sodium anode surface of P-GPE based full cell after 1000 cycles at 3 C. **(e)** voltage-capacity of PSB60-GPE based full cell at various rates. **(f)** Cycling performance of PSB60-GPE based full cell at 5 C. **(g)** Galvanostatic cycling of PSB60-GPE, P-GPE and LE based symmetric cells at 0.5 mA cm^{-2}. With permission from Ref. [166] copyrights 2023, Energy Storage Materials.

sults in improved conductivity (ionic), reaching 1.37 × 10^{-3} S/cm at 20 °C, and extends the electrochemical potential window of PSB60-GPE. PSB60-GPE-based symmetric cells exhibit stable cycling by 800 h at 0.5 mA/cm^2, exhibiting remarkable stability versus the Na^+ anode. Moreover, NVP/Na cells with PSB60-GPE demonstrate exceptional cyclic rate and efficiency at moderate temperatures.

Zhao and his team developed a customizable porous 3D network using PVDF-HFP and SnO_2. They refined the ionic conductivity pathway within the GPE by incorporating 1-(4-Cyanophenyl)-guanidines (CPg). The 3D network of PVDF-HFP facilitates the storage and movement of Na-ions, and the imino-N atom of CPg acts as a ligand, boosting the conduction of Na^+ ions through interaction. Fig. 11(a) illustrates the step-

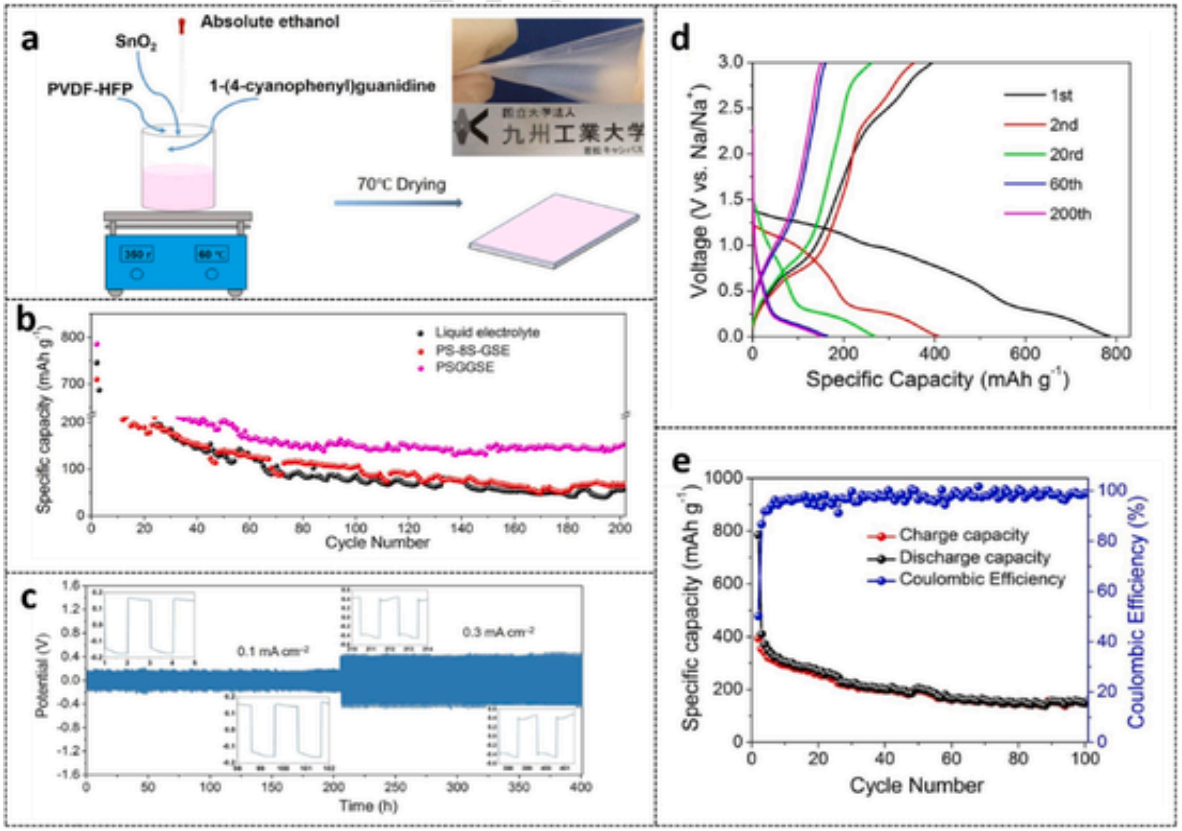

Fig. 11. (a) Synthetic strategy process of PSG membrane **(b)** Comparison of cycling performance of LE, PS-GSE, and PSGGSE at 100 mA/g between the range of 0.01–3.0 V **(c)** Voltage response of a Na/PSGGSE/Na symmetric battery upon galvanastic polarization **(d)** The charge and discharge profiles of PSSE for the 1st, 2nd, 20th, 60th, and 200th cycles at a current density of 100 mA/g. **(e)** Cycling performance of PSSE at 100 mA/g between the range of 0.01–3.0 V. With permission from Ref. [167] copyrights 2022, Chemical Engineering Journal.

by-step synthetic methodology employed to fabricate a porous 3D architectured polymer support matrix (PSG) [167]. Fig. 11(b) displays the GCD cyclic result of Na/PSGGSE/Na cells, showcasing the performance at current densities from 0.0001 A/cm^2 to 0.0003 mA/cm^2 under room temperature conditions. The Na/PSGGSE/Na batteries demonstrate consistent and reliable cycling behavior and commendable room temperature performance rates. Furthermore, even after prolonged cycling at room temperature, there were no short-circuiting instances, signifying the samples' excellent electrochemical stability. To examine the storage attributes with PE within the cell, a complete battery configuration comprising a Na^+ sheet, GPE, and $NiMoO_4$ electrode was assembled and subjected to electrochemical testing, as illustrated in Fig. 11. These comparative batteries utilized a LE, namely PS-8S-GSE, alongside PSGGSE. In Fig. 11(c), it is showcased that the PSGGSE-utilizing battery showcased superior electrochemical performance compared to the battery equipped with the LE. Fig. 11(d) illustrates the GCD curves conducted at 0.05 A/g within a potential range of 0.01–3.0 V (vs Na/Na^+). Initially, the C_{sp} was done at 785.6 mAh/g. The reduction in irrevocable capacity and the low CE are likely due to the formation of the SEI membrane and the presence of undecomposed Na_2O. Throughout cycling, the discharge capacities for the first, second, 20th, sixty, and 200th cycles were recorded at 785.6, 409.6, 269, 163.9, and 152.3 mAh/g, respectively. Subsequent GCD profiles after the initial cycle exhibited similar shapes. However, a gradual decrease in discharge capacity occurred with an increasing cycle count. Fig. 11(e) shows the cyclic performance of the $NiMoO_4$ electrode under multiple current densities. Before the 40th cycle, there was a rapid capacity decline notably. However, the electrode material displayed stable capacities after the 80th cycle, signifying exceptional recovery and consistent reversible electrochemical cyclic ability. To delve deeper into understanding the remarkable performance of PSGGSE, they analyzed the $NiMoO_4$ anode's morphology at around 200 cycles. Additionally, they explored the potential of polymer membranes to uphold the architectural firmness of the anode. Fig. 12(a) and (b) present SEM results of the $NiMoO_4$-based anode before initiating the cycling process. In contrast, Fig. 12(c) and (d) showcase SEM images of $NiMoO_4$ based anode immersed in the LE. Meanwhile, Fig. 12(e) and (f) display SEM results of the $NiMoO_4$ anode within the PSGGSE electrolyte. Notably, this anode depicted a flat surface after 200 cycles when using the SE without exhibiting any discernible cracks. In contrast, the $NiMoO_4$ anode subjected to the LE displays an uneven surface post-200 cycles, showing severe fragmentation with powder material accumulating within the cracks. This stark contrast underscores the ability of the SE to keep the architectural integrity of the anode, contributing to its enhanced performance.

In conclusion, incorporating SnO_2 resulted in a melodious porous architecture and ameliorated interface stability. The addition of CPg increased Na^+ transport sites. PSGGSE displayed high ionic conductivity and robust cyclic performance (Na/PSGGSE/Na). It effectively suppressed Na^+ dendrite growth after over 400 h of cycling in symmetric batteries. Na/PSGGSE/$NiMoO_4$ batteries also achieved a C_{sp} surpassing LE performance. SEM analysis post-cycling revealed a stable PSGGSE/anode interface, mitigating electrode material pulverization from volume expansion during charge/discharge. These findings hold promise for advancing Na-ion SE research.

Saroja et al. created a GPE by incorporating hydroxyapatite, a calcium phosphate-based compound, into a PVDF-HFP-PBMA blend membrane (HAP-GPE), employing a simple solution-casting technique [168]. The as-prepared membrane has an ionic conductivity of 0.001086 S cm^{-1}, good porosity, electrolyte absorption, and electrochemical stability by 4.9 V. Because of these qualities; it is an excellent electrolyte for rechargeable NIBs. The CV, GCD, and EIS characteristics of $Na_3V_2(PO_4)_3$/C (NVP/C) were studied utilizing the synthesized GPE to showcase its viability. The GCD results of NVP/C at different C-rates within the potential range of 2.2–3.8 V are shown in Fig. 13(a). The GCD data displays a distinct peak representing the conservation reaction from $Na_3V_2(PO_4)_3$ to $NaV_2(PO_4)_3$, associated with V^{4+}/V^{3+} redox reactions. At 0.1 C, the C_{sp} of NVP/C with the HAP/GPE membrane with 136 mAhg^{-1} of C_{sp}. Comparatively, at the same rate, the cell used GF as a separator and 110 mAhg^{-1} C_{sp} (Fig. 13(b)). Using the NVP/C membrane, the C_{sp} for the NVP/C cathode shows a 23.6 % improvement over the GF membrane. Na-ion cells with GPE and GF membranes are evaluated cyclically at 1 C. Retaining 92.7 % of its capacity by 100 cycles, the HAP/GPE membrane-equipped cell shows exceptional stability, whereas the GF membrane shows 88.3 % retention. The HAP/GPE membrane cell-equipped cell maintains roughly 71.7 % of its capacity after 500 cycles. The lower capacitance retention in the cell with the GF membrane is attributed to cell polarization, consistent with the GCD profile showing larger over-potential values (Fig. 13(c and d)).

Moreover, the decent electrochemical stability, low Na^+ ion transference number, and higher ionic conductivity contribute to the superior electrochemical behavior of the NVP/C cathodes with the HAP-GPE membrane compared to the GF separator. The enhanced electrochemi-

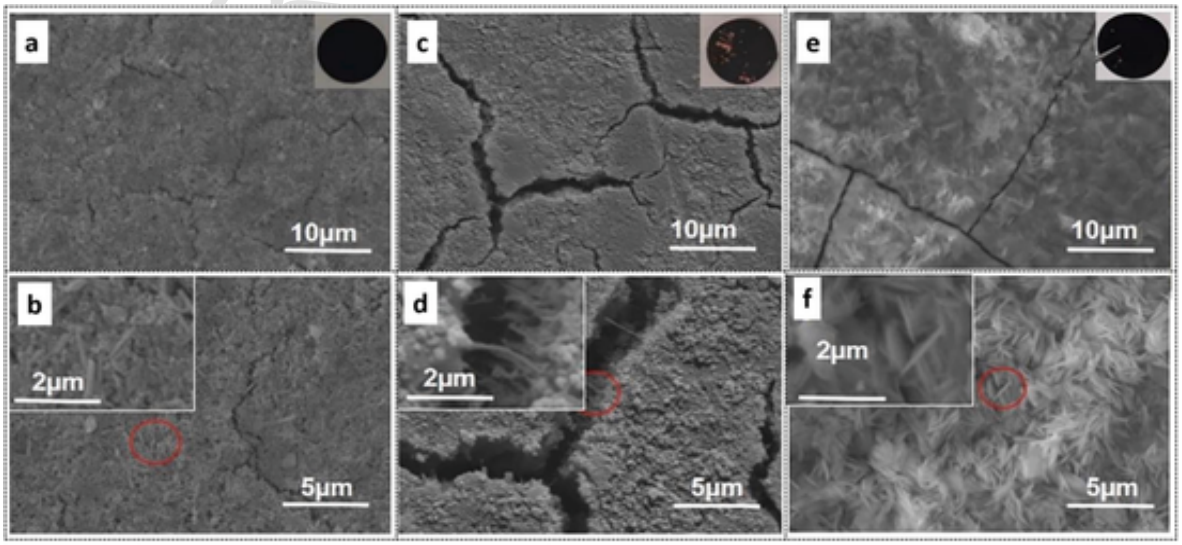

Fig. 12. SEM images of **(a), (b)** anode electrode before test cycle performance **(c), (d)** liquid electrolyte anode electrode after test cycle performance. (e), (f) PSGGSE anode electrode after test cycle performance. With permission from Ref. [167] copyrights 2022, Chemical Engineering Journal.

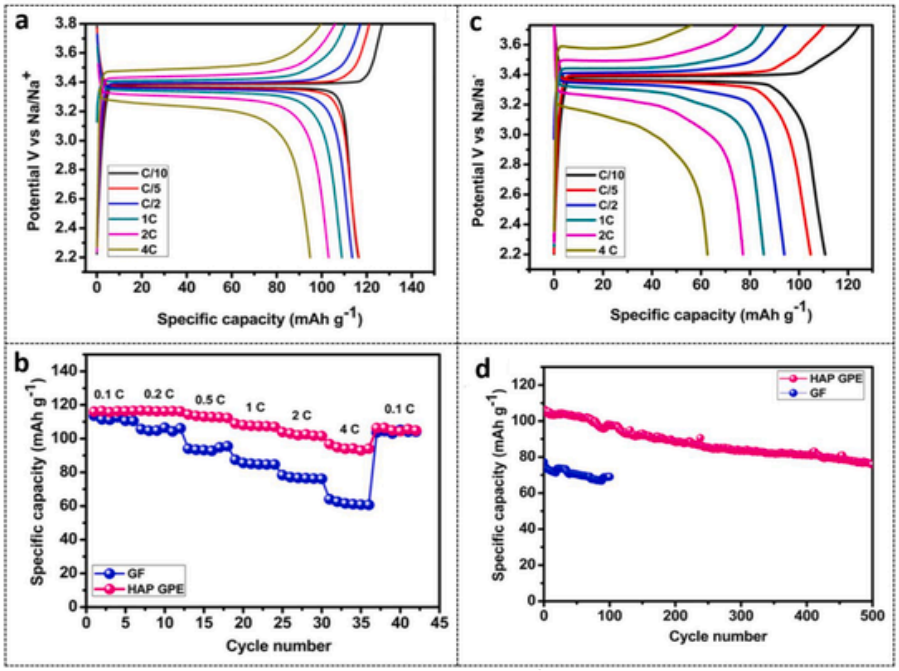

Fig. 13. Galvanostatic charge-discharge curves of NVP/C using **(a)** HAP-GPE, **(c)** GF, (b) rate capability, **(d)** cyclic stability of NVP/C cathode using GF and HAP-GPE. With permission from Ref. [168] copyrights 2020, Journal of Electroanalytical Chemistry.

cal properties of the NIB employing the HAP-GPE membrane at room temperature hold the potential for advancing high-performance and safer battery technologies. Chen et al. fabricated a flexible PPEGMA-based GPE (PGT32-5%) through an in-situ thermal-cured method. The non-flammable triethyl phosphate plasticized the electrolyte and was reinforced with GF support [169]. The optimized anti-flame electrolyte of PGT32-5% demonstrates excellent characteristics with a high ionic conductivity of 0.91 mS cm^{-1} at 27 °C and a wide electrochemical window of 4.8 V. An artificial interface was intentionally established by the polymer, and the Na^+ anode to ensure superior cyclic stability. The quasi-solid-state $Na_3V_2(PO_4)_3$/PGT32-5%/Na (NVP/PGT32-5%/Na) battery exhibited remarkable performance, retaining 91 % of its capacity after 400 cycles [170]. The electrochemical performance of PGT32-5 % in NIBs at room temperature was assessed using NVP|PGT32-5%|Na half-cell. As depicted in Fig. 14(a), NVP|PGT32-5%|Na initially exhibits a discharge/charge capacity of 105.3/117.2 $mAhg^{-1}$ at 0.1C. The plateaus observed align with two oxidation peaks and one reduction in the CV curves (Fig. 14(b)), and these features remain relatively stable in successive cycles, mitigating unwanted side reactions throughout observable cycling [171]. At the current density of 0.2 C, NVP|PGT32-5%|Na demonstrates 102 $mAhg^{-1}$ of initial discharge capacity, maintaining a higher capacity retention of 91 % after 400 cycles (Fig. 14(c)). This underscores a substantial enhancement in cycling stability while the GPEs contain 5 % of FEC. The rate performance of NVP|PGT32-5%|Na at various current densities is noteworthy (Fig. 14 (d)). The cell exhibits 102.9, 100, 95.9, 92.3, 86.3, and 80 $mAhg^{-1}$ capacities at 0.1, 0.2, 0.5, 1, 2, and 3C, respectively. Furthermore, the capacity remains high at 98.7 $mAhg^{-1}$ when the current density returns to 0.2 C. This emphasizes the robust performance of the NVP|PGT32-5%|Na system across a range of charging and discharging rates.

In comparison, the self-supported GPE, PGT32-5%, exhibits a higher ionic conductivity of 9.1 × 10^{-4} S/cm and elevated oxidation degradation potential of 4.8 V (vs. Na^+/Na) with superb flexibility. Adding FEC ensures a stable interface, protecting the Na^+ metal anodes by TEP and leftover PEGMA corrosion [172]. This stable interface enables NVP|PGT32-5%|Na quasi-solid-state NIBs to show high retention. Additionally, insights into the composition of the interface and voltage anomalies provide valuable guidance for constructing electrode/electrolyte interface stabilities incorporated by interface battery chemistry.

In their study, Wang et al. prepared Na-supported $Na_3Zr_2Si_2PO_{12}$ NPs mutated by PVDF-HFP/PMMA/TPU (PHPT) based GPEs and demonstrated their performance in NIBs [170]. Increased uptake of LE results from inserting $Na_3Zr_2Si_2PO_{12}$ filler, which decreases the crystallinity of polymer matrices and increases the GPE membrane's porosity. This resulted in an increased ionic conductivity, up to 0.00283 Scm^{-1}, of these $Na_3Zr_2Si_2PO_{12}$-modified GPEs with an extended electrochemical stability potential of 5.16 V and comparatively lower activation energy of nearly 0.039 eV. The GPE membranes based on PHPT containing 0, 2, 4, 6, and 8 wt% of $Na_3Zr_2Si_2PO_{12}$ NPs were labeled as GPE-0, GPE-II, GPE-IV, GPE-VI, and GPE-VIII, following. Porosity analysis of SEM findings of the GPEs was conducted using Image J software and is shown in Fig. 15(a–e) it is beneficial for ionic conductivity that the GPE membranes have a porous design. This structure facilitates the storage of LEs and provides a pathway for the movement of Na ions. It is evident from the images that the GPE-0 membrane had only a few small holes. However, the size and density of pores in the GPEs increased once the $Na_3Zr_2Si_2PO_{12}$ filler was added. The porosity values were found to be (0.0707 × 10^2)%, (0.1498 × 10^2)%, (0.2871 × 10^2)%, (0.1234 × 10^2)%, and (0.1016 × 10^2)% for the GPE(0- VIII) membranes, respectively. Exceeding the optimal number of fillers led to NP agglomeration in a polymer matrix, decreasing porosity. The DC polarization technique was consequently concerned with determining the Na-ion tNa^+ of the GPE-0 and GPE-4 membranes. Not only did the ion-conducting filler raise the percentage of Na^+ ions, but it also improved LE absorption, which made it easier for Na^+ ions to migrate. Consequently, GPE-4 exhibited a greater tNa^+ value of 0.63 than GPE-0 (0.33). Fig. 16(c) shows Na|GPE-0|Na and Na|GPE-4|Na, GCD cycling curves of symmetrical cells at 0.0005 A cm^{-2}. It is important that the symmetric Na|GPE-4|Na cell exhibited a lower and better polarization voltage than the symmetric Na|GPE-0|Na cell, showing that the ion-conducting filler plays a role in creating a stable electrolyte/electrode interface. The performance of the fabricated GPE

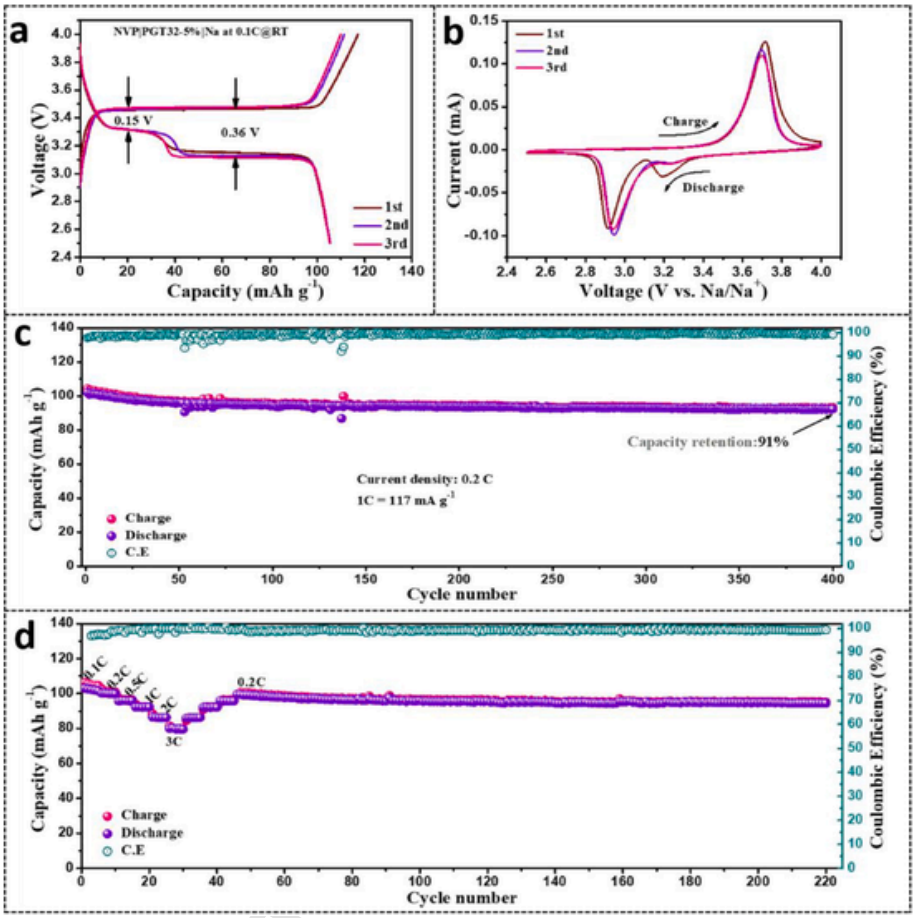

Fig. 14. Electrochemical performances of NVP|PGT32-5%|Na cells at room temperature **(a)** Charge and discharge curves at a current density of 0.1C, **(b)** cyclic voltammetry curves, **(c)** cycling performance at 0.2C, **(d)** rate performance at a current density range from 0.1C to 3C. With permission from Ref. [169] copyrights 2020, Chemical Engineering Journal.

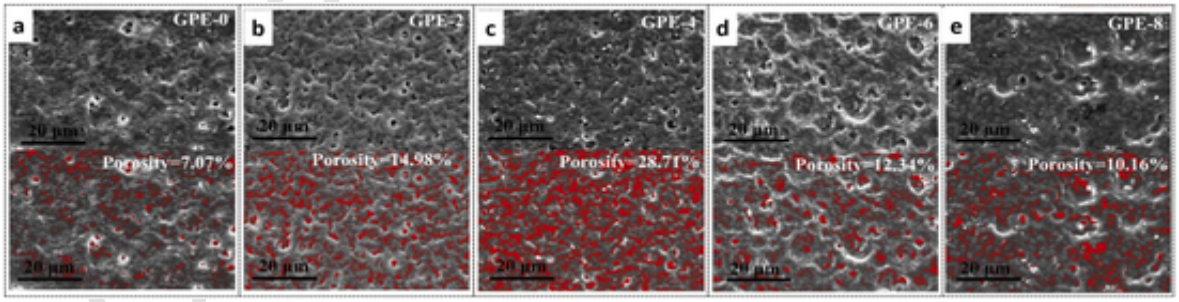

Fig. 15. SEM images associated with the porosity analysis using the Image J software for the obtained **(a)** GPE-0; **(b)** GPE-2; **(c)** GPE-4; **(d)** GPE-6; and **(e)** GPE8 membranes. With permission from Ref. [170] copyrights 2021, Solid State Ionics.

membranes in NIBs was assessed by evaluating the electrochemical characteristics of $Na_3V_2(PO_4)_3$/C|GPEs|Na batteries, as depicted in Fig. 16(d–g). The cyclic capability of the $Na_3V_2(PO_4)_3$/C|GPEs|Na cell assembled at 0.5C is shown in Fig. 16(d). Initially, the discharge-specific capacities were measured as 88.8, 92.1, 92.7, 90.9, and 90.6 $mAhg^{-1}$, which corresponds to GPE-0, GPE-II, GPE-IV, GPE-VI, and GPE-VIII samples. At the end of 100 cycles, the discharge capacities were 85.0, 90.9, 92.0, 90.1, and 89.8 $mAhg^{-1}$, at capacitance retentions of (0.957×10^2)%, (0.987×10^2)%, (0.992×10^2)%, (0.991×10^2)%, and (0.991×10^2)%, respectively. Fig. 16(e) depicts the typical charge and discharge curves associated with $Na_3V_2(PO_4)_3$/C|GPE-4|Na cell, assembled at 0.5 C. The charge/discharge curves showed two platforms at ~3.4 V (vs. Na/Na^+) and ~3.3 V (vs. Na/Na^+), respectively. These platforms correspond to the reversible oxidative change from V^{3+} to V^{4+} associated with its extraction and incorporation of Na^+ ions in cathodes of $Na_3V_2(PO_4)_3$. Fig. 16(f) depicts the performance rates of $Na_3V_2(PO_4)_3$/C|GPE-0|Na and $Na_3V_2(PO_4)_3$/C|GPE-4|Na batteries at multiple current density values. The typical charge/discharge curves of the $Na_3V_2(PO_4)_3$/C|GPE-4|Na battery at various current densities are illustrated in Fig. 16(g). Clear observation of these two platforms was

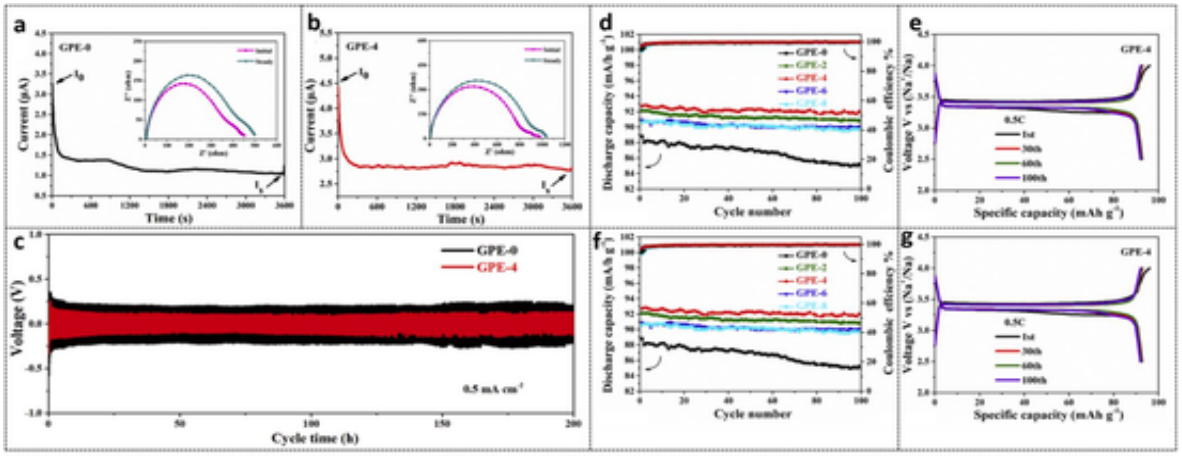

Fig. 16. Current-time profiles and the electrochemical impedance spectra before and after polarization for the assembled **(a)** Na|GPE-0|Na; **(b)** Na|GPE-4|Na symmetrical cells under a polarization voltage of 10 mV; **(c)** Galvanostatic cycling curves of Na|GPE-0|Na and Na|GPE-4|Na symmetrical cells at the current density of 0.5 $mAcm^{-2}$ **(d)** Cycling performance of the assembled $Na_3V_2(PO_4)_3$/C|GPEs|Na batteries at 0.5C; **(e)** Typical charge/discharge curves of the assembled $Na_3V_2(PO_4)_3$/C| GPE-4|Na battery at 0.5 C **(f)** The rate performance of the assembled $Na_3V_2(PO_4)_3$/C|GPE-0|Na and $Na_3V_2(PO_4)_3$/C|GPE-4|Na battery at various current densities; **(g)** Typical charge/discharge curves of the assembled $Na_3V_2(PO_4)_3$/C|GPE-4|Na battery at various current densities. With permission from Ref. [170] copyrights 2021, Solid State Ionics.

possible when the cell was charged and discharged with a small current. However, under successive higher current densities, the same platforms became less distinct because of the slow diffusion of Na^+. Table 4 explains the electrochemical properties of GPE composites for the NIBs.

In wrap-up, these systems for NIBs and GPEs made from PVDF-HFP are widely used. When these electrolyte membranes are made into NFs using electrospinning, they become more porous [173]. This higher porosity helps ions move more efficiently, increasing conductivity. Adding tiny particles called nanofillers to these GPEs and coating them onto a common separator also strengthens conductivity. Another promising approach involves creating polymer hosts through in situ polymerization using materials related to PEO and PMMA. These polymer hosts have excellent properties, especially in terms of strength and stability at the interfaces within the battery. They can prevent the formation of harmful structures called sodium dendrites, improving battery performance over many charging cycles. GPEs made with these crosslinked polymers show great potential for use in NIBs.

Additionally, flame-retardant materials, such as certain chemicals or special polymers, can enhance their thermal stability and safety in GPEs [174]. Another approach involves using a type of PE that only allows one type of ion to move, minimizing a phenomenon called polarization during charging and discharging. Combining these different strategies can further improve the performance of GPEs, making it promising to create ideal ones through optimization and combination [175].

Table 4
Electrochemical properties of Gel polymer electrolytes composites for Na-ion batteries.

Composite	Capacity (mAh/g)	Current density	No. of cycles	Retention	Columbic efficiency	ref
GF/PVDF-HFP/PDA membrane	131.1	0.2 C	100	89.4 %	98.4 %	[1]
GPE-CPN	85	–	50	85.8 %	–	[2]
PVDF–HFP	93.6	3 C	1000	92.2 %	99.9 %	[3]
PSGGSE	785.6	50 mA/g	200	34 %	–	[4]
$Na_3V_2(PO_4)_3$/C	97	4 C	500	91.8 %	–	[5]
NVP|PGT32-5%|Na	105.3	0.1C	400	91 %	–	[6]
$Na_3V_2(PO_4)_3$	111.9	0.2 C	100	100 %	99.5 %	[8]
Na/GPE/$Na_3V_2(PO_4)_2F_3$	106.7	0.1 mA/cm^2	100	93	–	[9]
Na/NWPH-GPE/PB@rGO	104.6	1 C	1000	96	99.5 %	[10]
$Na_3Zr_2Si_2PO_{12}$	92.7	0.5C	100	99.2 %	–	[7]
P(VdF-co-HFP)	118.99	0.1C	50	97 %	–	[11]
$Na_3V_2(PO_4)_3$/Na	117.8	1 C	500	89.6 %	~100 %	[12]
$Na_3V_2(PO_4)_3$	114.9	1 C	1100	96 %	99.9 %	[13]
GPE/Na–Hg/P–C	225	31 mA/g	–	55 %	–	[14]
PI/MWCNT	98	5 C	3000	84 %	–	[15]
HC|PAN_5%M|Na	200	20 C	10	88.8 %	98.7 %	[16]
$Na_3V_2(PO_4)_3$/GPEs/Na	87.5	0.5C	300	95.1 %	96.3 %	[17]
$Na_3V_2(PO_4)_3$/C|GPE|Na	92.3	0.5C	100	98.18 %	–	[18]

8. Challenges and future outlook

The current generation of SSEs GPEs requires further enhancement and optimization. While some GPEs show lower ionic conductivities at room temperature, most possess conductivities exceeding 10^{-4} S/cm, suitable for charge-storing applications. Ensuring the mechanical robustness of GPEs is crucial for suppressing sodium dendrite formation and accommodating various electrode materials [176]. Despite this, pure GPE membranes often lack sufficient mechanical strength to form self-standing membranes, hindering their practical utility. Enhancing the intrinsic safety of GPEs is essential. While GPEs reduce the chances of liquid leakage and inhibit sodium dendrites' growth, they still exhibit inadequate fire resistance because of combustible liquid plasticizers and polymer matrices. Common approaches to improving flame retardance include incorporating functional anti-flame additives, utilizing non-flammable liquids like plasticizers, or directly employing anti-flame polymer hosts. The interactions at the interface between GPEs and electrodes necessitate thorough exploration using diverse characterization methods, including advances in situ techniques and theoretical modeling base. Establishing suitable electrolyte/electrode interfaces is crucial for ensuring the long-term cyclic stability associated with NIBs [177]. Despite considerable efforts to elucidate interface phenomena and the formation of the SEI, the literature on NIBs needs to catch up to that of LIBs. Existing studies primarily address the interface between SSEs and sodium metal anodes. Further investigations are required to understand the internal reaction mechanisms at these interfaces, including interactions with various electrode materials. Develop-

ing effective strategies to enhance interface compatibility beyond conventional film-forming additives remains a formidable challenge [178–180].

GP NIBs have made progress but face challenges for practical use. Few GPE-based NIBs exceed 1000 cycles, especially with HC and non-$Na_3V_2(PO_4)_3$ materials [181]. Full cell performance needs improvement as they bridge laboratory and commercial packs. Experimental conditions for testing are vital for real-world use. Electrolyte and electrode development must align to commercialize NIBs effectively. Designing environment-friendly electrode materials, like Iron, carbon, or organic framework-based materials, as a substitute for toxic metals like Co and V is crucial. This study's essentials are optimizing storage capacity at a suitable working voltage, enhancing system stability, and matching suitable GPE. Combining GPEs with eco-friendly electrodes can broaden their applications.

9. Conclusion

Humanity faces urgent energy and atmosphere challenges, requiring the development of clean and green energy sources. This includes the need for low-cost, long-lasting stationary ESDs to manage the intermittent output of renewable sources. Rechargeable NIBs are gaining attention as alternatives to LIBs due to their natural abundance and lower cost. GPE systems are being developed to improve safety and performance, offering benefits such as reduced electrolyte decomposition, enhanced safety, and extended battery life compared to conventional LEs. GPEs are receiving increased attention because of their promising attributes, such as higher standard temperature ionic conductivity, border electrochemical windows, better thermal stability, decent mechanical properties, and reliability as electrodes during cycling. We first examine the architectural execution relationships of these polymer matrices. Then, the critical parameters for evaluating GPEs with a discussion of the factors influencing them, along with improvement measures, are reported. We also review approaches to optimize electrochemical performance and analyze ion transport pathways and conduction mechanisms. Lastly, we discuss efforts to establish advanced GPE systems with enhanced properties, including electrochemical windows, ionic conductivity, flame retardancy, thermal stability, mechanical strength, and interfacial stability. PVDF-HFP-based GPEs and their constituents are broadly used in NIBs, with electrospun nanofibrous membranes increasing ionic conductivity and ion transportation. Coating or adding nanofillers in separators further enhances conductivity and mechanical properties. In situ polymerized GPEs with crosslinking frameworks show potential for SIBs. Flame-retardant GPEs using non-flammable additives or polymer frameworks improve thermal stability. Single-ion conducting polymer electrolytes reduce polarization during cycling, enhancing ion transfer efficiency. Combining these strategies can further boost performance, suggesting promising avenues for optimizing GPEs.

Uncited references

[115].

CRediT authorship contribution statement

Farooq Ahmad: Writing – review & editing, Writing – original draft, Methodology, Conceptualization. **Amir Shahzad:** Writing – review & editing, Methodology, Investigation. **Saira Sarwar:** Software, Resources, Methodology. **Hina Inam:** Visualization, Validation, Resources, Data curation. **Umer Waqas:** Writing – review & editing, Investigation. **Dawid Pakulski:** Writing – review & editing, Supervision, Methodology, Conceptualization. **Michal Bielejewski:** Validation, Software, Formal analysis, Data curation. **Shahid Atiq:** Writing – review & editing, Supervision, Project administration. **Sania Amjad:** Validation, Software, Resources, Conceptualization. **Muhammad Irfan:** Formal analysis, Conceptualization. **Hadia Khalid:** Formal analysis, Data curation. **Muhammad Adnan:** Software, Resources. **Osama Gohar:** Visualization, Validation.

Declaration of competing interest

The authors declare that they have no known competing financial interests or personal relationships that could have appeared to influence the work reported in this paper.

Data availability

Data will be made available on request.

References

[1] H. Li, Z. Xu, J. Yang, J. Wang, S.I. Hirano, Polymer electrolytes for rechargeable lithium metal batteries, Sustain. Energy Fuels 4 (2020).
[2] D.K. Maurya, R. Dhanusuraman, Z. Guo, S. Angaiah, Composite polymer electrolytes: progress, challenges, and future outlook for sodium-ion batteries, Adv. Compos. Hybrid Mater. 5 (2022).
[3] P.K. Nayak, L. Yang, W. Brehm, P. Adelhelm, From lithium-ion to sodium-ion batteries: advantages, challenges, and surprises, Angew. Chem. Int. Ed. 57 (2018).
[4] K. Chayambuka, G. Mulder, D.L. Danilov, P.H.L. Notten, From Li-ion batteries toward Na-ion chemistries: challenges and opportunities, Adv. Energy Mater. 10 (2020).
[5] Y. Huang, Y. Zheng, X. Li, F. Adams, W. Luo, Y. Huang, L. Hu, Electrode materials of sodium-ion batteries toward practical application, ACS Energy Lett. 3 (2018).
[6] Q. Yang, Z. Zhang, X.G. Sun, Y.S. Hu, H. Xing, S. Dai, Ionic liquids and derived materials for lithium and sodium batteries, Chem. Soc. Rev. 47 (2018).
[7] J. Pan, N. Wang, H.J. Fan, Gel polymer electrolytes design for Na-ion batteries, Small Methods 6 (2022).
[8] X. Guo, Z. Xie, R. Wang, J. Luo, J. Chen, S. Guo, G. Tang, Y. Shi, W. Chen, Interface-compatible gel-polymer electrolyte enabled by NaF-Solubility-Regulation toward all-climate solid-state sodium batteries, Angew. Chem. Int. Ed. 63 (2024) e202402245.
[9] L. Zhang, X. Li, M. Yang, W. Chen, High-safety separators for lithium-ion batteries and sodium-ion batteries: advances and perspective, Energy Storage Mater. 41 (2021) 522–545.
[10] X. Li, J. Zhang, X. Guo, C. Peng, K. Song, Z. Zhang, L. Ding, C. Liu, W. Chen, S. Dou, An ultrathin nonporous polymer separator regulates Na transfer toward dendrite-free sodium storage batteries, Adv. Mater. 35 (2023) 2203547.
[11] A. Gabryelczyk, H. Smogór, A. Swiderska-Mocek, Highly conductive gel polymer electrolytes for sodium-ion batteries with hard carbon anodes, Electrochim. Acta 439 (2023).
[12] O.V. Lonchakova, O.A. Semenikhin, M.V. Zakharkin, E.A. Karpushkin, V.G. Sergeyev, E.V. Antipov, Efficient gel-polymer electrolyte for sodium-ion batteries based on poly(acrylonitrile-co-methyl acrylate), Electrochim. Acta 334 (2020).
[13] H. Gao, W. Zhou, K. Park, J.B. Goodenough, A sodium-ion battery with a low-cost cross-linked gel-polymer electrolyte, Adv. Energy Mater. 6 (2016).
[14] F. Ahmad, A. Shahzad, M. Danish, M. Fatima, M. Adnan, S. Atiq, M. Asim, M.A. Khan, Q.U. Ain, R. Perveen, Recent developments in transition metal oxide-based electrode composites for supercapacitor applications, J. Energy Storage 81 (2024) 110430.
[15] M. Saleem, F. Ahmad, M. Fatima, A. Shahzad, M.S. Javed, S. Atiq, M.A. Khan, M. Danish, O. Munir, S.M.B. Arif, Exploring new frontiers in supercapacitor electrodes through MOF advancements, J. Energy Storage 76 (2024) 109822.
[16] F. Ahmad, M. Asim, S. Mubashar, A. Shahzad, Q.U. Ain, M.A. Khan, S. Atiq, M. Adnan, H. Jamil, A. Qayyum, Revolutionizing energy storage: a critical appraisal of MXene-based composites for material designing and efficient performance, J. Energy Storage 84 (2024) 110757.
[17] K. Mizushima, P.C. Jones, P.J. Wiseman, J.B. Goodenough, $LixCoO_2$ (0, Solid State Ionics 3–4 (1981).
[18] A. Mendiboure, C. Delmas, P. Hagenmuller, Electrochemical intercalation and deintercalation of $NaxMnO_2$ bronzes, J. Solid State Chem. 57 (1985).
[19] A. Yoshino, The birth of the lithium-ion battery, Angew. Chem. Int. Ed. 51 (2012), https://doi.org/10.1002/anie.201105006.
[20] A. Van Zyl, Review of the zebra battery system development, Solid State Ionics 86–88 (1996).
[21] D.A. Stevens, J.R. Dahn, High capacity anode materials for rechargeable sodium-ion batteries, J. Electrochem. Soc. 147 (2000).
[22] Y.S. Hu, S. Komaba, M. Forsyth, C. Johnson, T. Rojo, A new emerging technology: Na-ion batteries, Small Methods 3 (2019).
[23] Y. Zhu, Y. Yang, L. Fu, Y. Wu, A porous gel-type composite membrane reinforced by nonwoven: promising polymer electrolyte with high performance for sodium ion batteries, Electrochim. Acta 224 (2017).
[24] J. Pan, N. Wang, H.J. Fan, Gel polymer electrolytes design for Na-ion batteries, Small Methods 6 (2022).
[25] D.H. Lim, M. Agostini, J.H. Ahn, A. Matic, An electrospun nanofiber membrane as gel-based electrolyte for room-temperature sodium–sulfur batteries, Energy

Technol. 6 (2018).
[26] N. Zhu, K. Zhang, F. Wu, Y. Bai, C. Wu, Ionic liquid-based electrolytes for aluminum/magnesium/sodium-ion batteries, Energy Mater. Adv. (2021).
[27] E. Matios, Sodium Batteries with Solid Electrolytes: Nanoscale Engineering, Composition Optimization and Structure-Property Correlation, Dartmouth College, 2021.
[28] X. Yang, A.L. Rogach, Anodes and sodium-free cathodes in sodium ion batteries, Adv. Energy Mater. 10 (2020) 2000288.
[29] M. Li, Z. Du, M.A. Khaleel, I. Belharouak, Materials and engineering endeavors towards practical sodium-ion batteries, Energy Storage Mater. 25 (2020) 520–536.
[30] W. Lu, Z. Wang, S. Zhong, Sodium-ion battery technology: advanced anodes, cathodes and electrolytes, J. Phys.: Conf. Ser. IOP Publ. (2021) 012004.
[31] N. Yabuuchi, K. Kubota, M. Dahbi, S. Komaba, Research development on sodium-ion batteries, Chem. Rev. 114 (2014) 11636–11682.
[32] T. Jin, H. Li, K. Zhu, P.-F. Wang, P. Liu, L. Jiao, Polyanion-type cathode materials for sodium-ion batteries, Chem. Soc. Rev. 49 (2020) 2342–2377.
[33] J.H. Stansby, N. Sharma, D.J. Goonetilleke, Probing the charged state of layered positive electrodes in sodium-ion batteries: reaction pathways, stability and opportunities, J. Mater. Chem. 8 (2020) 24833–24867.
[34] P. Hu, K.E. Aifantis, A.o.L.I. Design, Cells, beyond, Sodium-Ion Batteries, 2023, pp. 269–298.
[35] Y. Cao, M. Xiao, X. Sun, W. Dong, F. Huang, Recent advances on high-capacity sodium manganese-based oxide cathodes for sodium-ion batteries, Chem.--A Europ. J. 29 (2023) e202202997.
[36] R. Alcántara, C. Pérez-Vicente, P. Lavela, J.L. Tirado, A. Medina, R. Stoyanova, Review and new perspectives on non-layered manganese compounds as electrode material for sodium-ion batteries, Materials 16 (2023) 6970.
[37] X. Gao, W. Deng, G. Zou, H. Hou, X.S.-I.B.T. Ji, Applications, Cathode Materials of SIBs, 2023.
[38] F. Cheng, M. Cao, Q. Li, C. Fang, J. Han, Y. Huang, Electrolyte salts for sodium-ion batteries: napf6 or naclo4? ACS Nano 17 (2023) 18608–18615.
[39] G.G. Eshetu, G.A. Elia, M. Armand, M. Forsyth, S. Komaba, T. Rojo, S. Passerini, Electrolytes and interphases in sodium-based rechargeable batteries: recent advances and perspectives, Adv. Energy Mater. 10 (2020) 2000093.
[40] X. Zhu, L. Wang, Advances in materials for all-climate sodium-ion batteries, EcoMat 2 (2020) e12043.
[41] Z. Ouyang, Sodium-ion batteries: exploration of electrolyte materials, Highlight. Sci. Eng. Technol. 43 (2023) 419–426.
[42] J. Chen, A. Naveed, Y. Nuli, J. Yang, J. Wang, Designing an intrinsically safe organic electrolyte for rechargeable batteries, Energy Storage Mater. 31 (2020) 382–400.
[43] H. Dai, Y. Chen, W. Xu, Z. Hu, J. Gu, X. Wei, F. Xie, W. Zhang, W. Wei, R. Guo, A review of modification methods of solid electrolytes for all-solid-state sodium-ion batteries, Energy Technol. 9 (2021) 2000682.
[44] H. Ahmad, K.T. Kubra, A. Butt, U. Nisar, F.J. Iftikhar, G.J. Ali, Recent progress, challenges, and perspectives in the development of solid-state electrolytes for sodium batteries, J. Power Sources 581 (2023) 233518.
[45] H. Yin, C. Han, Q. Liu, F. Wu, F. Zhang, Y. Tang, Recent advances and perspectives on the polymer electrolytes for sodium/potassium-ion batteries, Small 17 (2021) 2006627.
[46] F. Gebert, J. Knott, R. Gorkin III, S.-L. Chou, S.-X. Dou, Polymer electrolytes for sodium-ion batteries, Energy Storage Mater. 36 (2021) 10–30.
[47] G. Chen, K. Zhang, Y. Liu, L. Ye, Y. Gao, W. Lin, H. Xu, X. Wang, Y. Bai, C. Wu, Flame-retardant gel polymer electrolyte and interface for quasi-solid-state sodium ion batteries, Chem. Eng. J. 401 (2020) 126065.
[48] D.K. Maurya, R. Dhanusuraman, Z. Guo, S.C. Angaiah, Composite polymer electrolytes: progress, challenges, and future outlook for sodium-ion batteries, Adv. Comp. Hybrid Mater. 5 (2022) 2651–2674.
[49] H. Verma, K. Mishra, D.J. Rai, Sodium ion conducting nanocomposite polymer electrolyte membrane for sodium ion batteries, J. Solid State Electrochem. 24 (2020) 521–532.
[50] M.S. Syali, K. Mishra, D. Kanchan, D.J. Kumar, Studies on a novel Na + superionic conducting polymer gel cocktail electrolyte membrane immobilizing molecular liquid mixture of carbonates, tetraglyme and ionic liquid, J. Molecular Liquid 341 (2021) 116922.
[51] N. Aslfattahi, L. Samylingam, M.S. Kiai, K. Kadirgama, V. Kulish, M. Schmirler, Z.J. Said, state-of-the-art review on electrolytes for sodium-ion batteries: potential recent progress and technical challenges, J. Energy Storage 72 (2023) 108781.
[52] K. Sirengo, A. Babu, B. Brennan, S.C.J. Pillai, Ionic liquid electrolytes for sodium-ion batteries to control thermal runaway, J. Energy Chem. (2023).
[53] C. Daniel, J.O. Besenhard, Handbook of Battery Materials, John Wiley & Sons, 2012.
[54] W. Zheng, W. Bi, Y. Fang, S. Chang, W. Yuan, L. Li, Solvent-free procedure to prepare ion liquid-immobilized gel polymer electrolytes containing li0.33la0.56tio3 with high performance for lithium-ion batteries, ACS Omega 6 (2021) 25329–25337.
[55] J.C. Barbosa, J.P. Dias, S. Lanceros-Méndez, C.M. Costa, Recent advances in poly (vinylidene fluoride) and its copolymers for lithium-ion battery separators, Membranes 8 (2018) 45.
[56] J. Zheng, W. Li, X. Liu, J. Zhang, X. Feng, W.J. Chen, Progress in gel polymer electrolytes for sodium-ion batteries, Energy Environ. Mater. 6 (2023) e12422.
[57] Y.-B. Niu, Y.-X. Yin, W.-P. Wang, P.-F. Wang, W. Ling, Y. Xiao, Y.-G. Guo, In situ copolymerizated gel polymer electrolyte with cross-linked network for sodium-ion batteries, CCS Chem. 2 (2020) 589–597.
[58] H. Gao, W. Zhou, K. Park, J.B. Goodenough, A sodium-ion battery with a low-cost cross-linked gel-polymer electrolyte, Adv. Energy Mater 6 (2016) 1600467.
[59] J.I. Kim, Y. Choi, K.Y. Chung, J.H. Park, A structurable gel-polymer electrolyte for sodium ion batteries, Adv. Funct. Mater 27 (2017) 1701768.
[60] A. Boschin, Sodium batteries: from liquid to polymer electrolytes, Chalmers Tekniska Hogskola (Sweden) (2016).
[61] K. Vignarooban, R. Kushagra, A. Elango, P. Badami, B.-E. Mellander, X. Xu, T. Tucker, C. Nam, A.M.J.I. Kannan, Current trends and future challenges of electrolytes for sodium-ion batteries, Int. J. Hydrogen Energy 41 (2016) 2829–2846.
[62] K. Deng, Q. Zeng, D. Wang, Z. Liu, Z. Qiu, Y. Zhang, M. Xiao, Y.J. Meng, Single-ion conducting gel polymer electrolytes: design, preparation and application, J. Mater. Chem. 8 (2020) 1557–1577.
[63] J. Zheng, X. Liu, Y. Duan, L. Chen, X. Zhang, X. Feng, W. Chen, Y.J. Zhao, Stable cross-linked gel terpolymer electrolyte containing methyl phosphonate for sodium ion batteries, J. Membr. Sci. 583 (2019) 163–170.
[64] J.I. Kim, K.Y. Chung, J.H.J. Park, Design of a porous gel polymer electrolyte for sodium ion batteries, J. Membr. Sci. 566 (2018) 122–128.
[65] J. Pan, N. Wang, H.J. Fan, Gel polymer electrolytes design for na-ion batteries, Small Method. 6 (2022) 2201032.
[66] L. Qiao, X. Judez, T. Rojo, M. Armand, H.J. Zhang, Polymer electrolytes for sodium batteries, J. Electrochem. Soc. 167 (2020) 070534.
[67] K. Mishra, N. Yadav, S.J. Hashmi, Recent progress in electrode and electrolyte materials for flexible sodium-ion batteries, J. Mater. Chem. 8 (2020) 22507–22543.
[68] Z.-Y. Li, Z. Li, J.-L. Fu, X. Guo, Sodium-ion conducting polymer electrolytes, Rare Metal. 42 (2023) 1–16.
[69] A.P.V.K. Saroja, A. Kumar, B.C. Moharana, M. Kamaraj, S.J. Ramaprabhu, Design of porous calcium phosphate based gel polymer electrolyte for quasi-solid state sodium ion battery, J. Electroanaly. Chem. 859 (2020) 113864.
[70] D. Lei, Y.-B. He, H. Huang, Y. Yuan, G. Zhong, Q. Zhao, X. Hao, D. Zhang, C. Lai, S. Zhang, Cross-linked beta alumina nanowires with compact gel polymer electrolyte coating for ultra-stable sodium metal battery, Nature 10 (2019) 4244.
[71] T. Jin, X. Ji, P.F. Wang, K. Zhu, J. Zhang, L. Cao, L. Chen, C. Cui, T. Deng, S. Liu, High-energy aqueous sodium-ion batteries, Angew. Chem. Int. Ed. 60 (2021) 11943–11948.
[72] L. Suo, O. Borodin, Y. Wang, X. Rong, W. Sun, X. Fan, S. Xu, M.A. Schroeder, A.V. Cresce, F. Wang, "Water-in-salt" electrolyte makes aqueous sodium-ion battery safe, green, and long-lasting, Adv. Energy Mater. 7 (2017) 1701189.
[73] H. Zhang, B. Qin, J. Han, S. Passerini, Aqueous/nonaqueous hybrid electrolyte for sodium-ion batteries, ACS Energy Lett. 3 (2018) 1769–1770.
[74] Z. Guo, Y. Zhao, Y. Ding, X. Dong, L. Chen, J. Cao, C. Wang, Y. Xia, H. Peng, Y. Wang, Multi-functional flexible aqueous sodium-ion batteries with high safety, Chem 3 (2017) 348–362.
[75] K. Nakamoto, R. Sakamoto, M. Ito, A. Kitajou, S. Okada, Effect of concentrated electrolyte on aqueous sodium-ion battery with sodium manganese hexacyanoferrate cathode, Electrochemistry 85 (2017) 179–185.
[76] J. Liu, C. Yang, B. Wen, B. Li, Y. Liu, Ultra-long cycle of prussian blue analogs achieved by equilibrium electrolyte for aqueous sodium-ion batteries, Small 19 (2023) 2303896.
[77] R.-S. Kühnel, D. Reber, C. Battaglia, A high-voltage aqueous electrolyte for sodium-ion batteries, ACS Energy Lett. 2 (2017) 2005–2006.
[78] H. Ao, C. Chen, Z. Hou, W. Cai, M. Liu, Y. Jin, X. Zhang, Y. Zhu, Y. Qian, Electrolyte solvation structure manipulation enables safe and stable aqueous sodium ion batteries, J. Mater. Chem. A 8 (2020) 14190–14197.
[79] Z. Hou, X. Li, J. Liang, Y. Zhu, Y. Qian, An aqueous rechargeable sodium ion battery based on a $NaMnO_2$–$NaTi_2(PO_4)_3$ hybrid system for stationary energy storage, J. Mater. Chem. A 3 (2015) 1400–1404.
[80] J.I. Kim, Y.G. Choi, Y. Ahn, D. Kim, J.H. Park, Optimized ion-conductive pathway in UV-cured solid polymer electrolytes for all-solid lithium/sodium ion batteries, J. Membr. Sci. 619 (2021) 118771.
[81] S. Vineeth, C.B. Soni, C. Sanjaykumar, Y. Yamauchi, M. Han, V. Kumar, A quasi-solid state polymer electrolyte for high-rate and long-life sodium-metal batteries, J. Energy Storage 73 (2023) 108780.
[82] J. Ma, X. Feng, Y. Wu, Y. Wang, P. Liu, K. Shang, H. Jiang, X. Hou, D. Mitlin, H. Xiang, Stable sodium anodes for sodium metal batteries (SMBs) enabled by in-situ formed quasi solid-state polymer electrolyte, J. Energy Chem. 77 (2023) 290–299.
[83] J.L. Olmedo-Martínez, A. Fdz De Anastro, M.a. Martínez-Ibañez, A.J. Müller, D. Mecerreyes, Polyethylene oxide/sodium sulfonamide polymethacrylate blends as highly conducting single-ion solid polymer electrolytes, Energy Fuel. 37 (2023) 5519–5529.
[84] J. Guo, F. Feng, S. Zhao, R. Wang, M. Yang, Z. Shi, Y. Ren, Z. Ma, S. Chen, T. Liu, Achieving ultra-stable all-solid-state sodium metal batteries with anion-trapping 3D fiber network enhanced polymer electrolyte, Small 19 (2023) 2206740.
[85] S. Hegde, V. Ravindrachary, G. Sanjeev, Ismayil, Characterization and charge transport properties of sodium ion conducting PEO: NaBr solid polymer electrolyte films, Polym. Eng. Sci. 63 (2023) 2468–2483.
[86] J. Pan, Y. Zhang, F. Sun, M. Osenberg, A. Hilger, I. Manke, R. Cao, S.X. Dou, H.J. Fan, Designing solvated double-layer polymer electrolytes with molecular interactions mediated stable interfaces for sodium ion batteries, Angew. Chem. 135 (2023) e202219000.
[87] L. Sahu, A. Bhatt, A. Chandra, A. Chandra, Hot-pressed sodium ion conducting solid polymer electrolytes: preparation and materials characterization, Mater. Today: Proc. (2023).
[88] K. Shu, J. Zhou, X. Wu, X. Liu, L. Sun, Y. Wang, S. Tian, H. Niu, Y. Duan, G. Hu, A PVDF/g– C_3N_4-based composite polymer electrolytes for sodium-ion battery, Polymers 15 (2023) 2006.

[89] C.S. Martinez-Cisneros, B. Pandit, B. Levenfeld, A. Varez, J.-Y. Sanchez, Flexible solvent-free polymer electrolytes for solid-state Na batteries, J. Power Sources 559 (2023) 232644.

[90] I. Hasa, S. Passerini, J. Hassoun, Characteristics of an ionic liquid electrolyte for sodium-ion batteries, J. Power Sources 303 (2016) 203–207.

[91] D. Zuo, L. Yang, Z. Zou, S. Li, Y. Feng, S.J. Harris, S. Shi, J. Wan, Ultrafast synthesis of NASICON solid electrolytes for sodium-metal batteries, Adv. Energy Mater. 13 (2023) 2301540.

[92] S. Wen, X. Li, J. Zhang, J. Wang, H. Ding, N. Zhang, D. Zhao, L. Mao, S. Li, Effects of sodium salts on compatibility between $Na_2Ti_3O_7$@ C anode and electrolyte for sodium-ion batteries, J. Alloys Compd. 930 (2023) 167380.

[93] R.H. DeBlock, C.-H. Lai, D.M. Butts, B.S. Dunn, Sodium-ion conducting pseudosolid electrolyte for energy-dense, sodium-metal batteries, J. Power Sources 554 (2023) 232305.

[94] M. Yang, F. Feng, Z. Shi, J. Guo, R. Wang, Z. Xu, Z. Liu, T. Cai, Z. Wang, C. Wang, Facile design of asymmetric flame-retardant gel polymer electrolyte with excellent interfacial stability for sodium metal batteries, Energy Storage Mater. 56 (2023) 611–620.

[95] H. Lai, Y. Lu, W. Zha, Y. Hu, Y. Zhang, X. Wu, Z. Wen, In situ generated composite gel polymer electrolyte with crosslinking structure for dendrite-free and high-performance sodium metal batteries, Energy Storage Mater. 54 (2023) 478–487.

[96] L. Ma, X. Li, J. Tan, Z. Fang, Z. Liu, Y. Wang, C. Ye, P. Yi, M. Ye, J. Shen, Anion-Immobilized gel polymer electrolyte with a high ion transference number for high-performance lithium/sodium metal batteries, ACS Appl. Mater. Interfaces (2023).

[97] P. Sehrawat, S. Parveen, S. Hashmi, High-performance sodium ion conducting gel polymer electrolyte based on a biodegradable polymer polycaprolactone, Energy Storage 5 (2023) e375.

[98] Q. Wang, X. He, Y. Wang, Y. Ma, D. Zhang, Z. Li, H. Sun, B. Wang, L.-Z. Fan, In-situ constructing efficient gel polymer electrolyte with fluoride-rich interface enabling high-capacity, long-cycling sodium metal batteries, Electrochim. Acta 465 (2023) 142968.

[99] Z. Zheng, X. Zhang, W. Shi, S. Liang, H. Cao, Y. Fu, H. Wang, Y. Zhu, AP (VDF-HFP) and nonwoven-fabric based composite as high-performance gel polymer electrolyte for fast-charging sodium metal batteries, Polymer 269 (2023) 125751.

[100] S. Das, S. Jana, M. Orságh, K. Byś, J. Mishra, M. Uchman, V. Adyam, Building sodium metal battery with polyisoprene-based air-stable single-ion gel polymer electrolyte, ACS Appl. Energy Mater. (2023).

[101] S. Parveen, S. Hashmi, Flexible gel polymer electrolyte comprising high flash point solvent adiponitrile with ethylene carbonate as co-solvent for sodium-ion batteries, J. Energy Storage 67 (2023) 107519.

[102] A. Gabryelczyk, H. Smogór, A. Swiderska-Mocek, Highly conductive gel polymer electrolytes for sodium-ion batteries with hard carbon anodes, Electrochim. Acta 439 (2023) 141645.

[103] A. Gabryelczyk, A. Swiderska-Mocek, D. Czarnecka-Komorowska, Muscovite as an inert filler for highly conductive and durable gel polymer electrolyte in sodium-ion batteries, J. Power Sources 552 (2022) 232259.

[104] A. Shahzad, F. Ahmad, S. Atiq, M. Saleem, O. Munir, M.A. Khan, S.M.B. Arif, Q.U. Ain, S. Sarwar, M. Asim, Harnessing the potential of MOF-derived metal oxide composites to optimize energy efficiency in batteries and supercapacitors, J. Energy Storage 87 (2024) 111447.

[105] S. Roberts, L. Chen, B. Kishore, C.E. Dancer, M.J. Simmons, E. Kendrick, Mechanism of gelation in high nickel content cathode slurries for sodium-ion batteries, J. Colloid Interface Sci. 627 (2022) 427–437.

[106] L. Staišiūnas, J. Pilipavičius, D. Tediashvili, J. Juodkazytė, L. Vilčiauskas, Engineering of conformal electrode coatings by atomic layer deposition for aqueous Na-Ion battery electrodes, J. Electrochem. Soc. 170 (2023) 050533.

[107] I. Mohsin U, L. Schneider, M. Häringer, C. Ziebert, M. Rohde, W. Bauer, H. Ehrenberg, H.J. Seifert, Heat generation and degradation mechanisms studied on Na3V2 (PO4) 3/C positive electrode material in full pouch/coin cell assembly, J. Power Sources 545 (2022) 231901.

[108] A. Kayyar, J. Huang, M. Samiee, J. Luo, Construction and testing of coin cells of lithium-ion batteries, JoVE 66 (2012) e4104.

[109] J. Seub Choi, Lee, H. Jin, Ha, J. Keun, K. Koo Cho, Synthesis and electrochemical properties of amorphous carbon coated Sn anode material for lithium-ion batteries and sodium ion batteries, J. Nanosci. Nanotechnol. 18 (2018) 15684.

[110] D. Ledwoch, D.J. Brett, E. Kendrick, The performance of hard carbon in a sodium ion battery and influence of the sodium metal in observed properties, ECS Trans. 72 (2016) 17.

[111] Y. Ma, Analyze the State of the Art of Lithiun-Ion and Sodium-Ion Batteries for Electric Vehicles, 2022.

[112] I. Nicotera, L. Coppola, C. Oliviero, M. Castriota, E. Cazzanelli, Investigation of ionic conduction and mechanical properties of PMMA–PVdF blend-based polymer electrolytes, Solid State Ionics 177 (2006) 581–588.

[113] J. Pan, N. Wang, H.J. Fan, Gel polymer electrolytes design for Na-ion batteries, Small Methods 6 (2022) 2201032.

[114] C.D. Zhao, J.-Z. Guo, Z.Y. Gu, X.-T. Wang, X.X. Zhao, W.H. Li, H.Y. Yu, X.L. Wu, Flexible quasi-solid-state sodium-ion full battery with ultralong cycle life, high energy density and high-rate capability, Nano Res. 15 (2022) 925–932.

[115] C. Costa, R. Leones, M.M. Silva, S. Lanceros-Mendez, Influence of different salts in poly (vinylidene fluoride-co-trifluoroethylene) electrolyte separator membranes for battery applications, J. Electroanal. Chem. 727 (2014) 125–134.

[116] W. Li, Y. Wu, J. Wang, D. Huang, L. Chen, G. Yang, Hybrid gel polymer electrolyte fabricated by electrospinning technology for polymer lithium-ion battery, Eur. Polym. J. 67 (2015) 365–372.

[117] Y. Wu, W. Zhong, W. Tang, L. Zhang, H. Chen, Q. Li, M. Xu, S.-j. Bao, Flexible electrode constructed by encapsulating ultrafine VSe2 in carbon fiber for quasi-solid-state sodium ion batteries, J. Power Sources 470 (2020) 228438.

[118] M.S. Park, H.S. Woo, J.M. Heo, J.M. Kim, R. Thangavel, Y.S. Lee, D.W. Kim, Thermoplastic polyurethane elastomer-based gel polymer electrolytes for sodium-metal cells with enhanced cycling performance, ChemSusChem 12 (2019) 4645–4654.

[119] Y. Zhang, Y. An, S. Dong, J. Jiang, H. Dou, X. Zhang, Enhanced cycle performance of polyimide cathode using a quasi-solid-state electrolyte, J. Phys. Chem. C 122 (2018) 22294–22300.

[120] J. Yang, M. Zhang, Z. Chen, X. Du, S. Huang, B. Tang, T. Dong, H. Wu, Z. Yu, J. Zhang, Flame-retardant quasi-solid polymer electrolyte enabling sodium metal batteries with highly safe characteristic and superior cycling stability, Nano Res. 12 (2019) 2230–2237.

[121] J.Z. Guo, A.B. Yang, Z.Y. Gu, X.L. Wu, W.L. Pang, Q.L. Ning, W.H. Li, J.P. Zhang, Z.M. Su, Quasi-solid-state sodium-ion full battery with high-power/energy densities, ACS Appl. Mater. Interfaces 10 (2018) 17903–17910.

[122] Y. Yang, Z. Chang, M. Li, X. Wang, Y. Wu, A sodium ion conducting gel polymer electrolyte, Solid State Ionics 269 (2015) 1–7.

[123] J. Manuel, X. Zhao, K.-K. Cho, J.-K. Kim, J.-H. Ahn, Ultralong life organic sodium ion batteries using a polyimide/multiwalled carbon nanotubes nanocomposite and gel polymer electrolyte, ACS Sustain. Chem. Eng. 6 (2018) 8159–8166.

[124] J. Pan, P. Zhao, N. Wang, F. Huang, S. Dou, Research progress in stable interfacial constructions between composite polymer electrolytes and electrodes, Energy Environ. Sci. 15 (2022) 2753–2775.

[125] M. Patel, R.K. Giri, K. Mishra, J. Chaudhari, D. Kanchan, P.K. Singh, D. Kumar, Synthesis and assessment of novel Na_2S dispersed high performance nanocomposite gel polymer electrolyte intended for sodium batteries and electric double layer capacitors, J. Energy Storage 86 (2024) 111280.

[126] M. Cheng, T. Qu, J. Zi, Y. Yao, F. Liang, W. Ma, B. Yang, Y. Dai, Y. Lei, A hybrid solid electrolyte for solid-state sodium ion batteries with good cycle performance, Nanotechnology 31 (2020) 425401.

[127] Q. Yu, Q. Lu, X. Qi, S. Zhao, Y.-B. He, L. Liu, J. Li, D. Zhou, Y.-S. Hu, Q.-H. Yang, Liquid electrolyte immobilized in compact polymer matrix for stable sodium metal anodes, Energy Storage Mater. 23 (2019) 610–616.

[128] H. Gao, B. Guo, J. Song, K. Park, J.B. Goodenough, A composite gel–polymer/glass–fiber electrolyte for sodium-ion batteries, Adv. Energy Mater. 5 (2015) 1402235.

[129] J.I. Kim, K.Y. Chung, J.H. Park, Design of a porous gel polymer electrolyte for sodium ion batteries, J. Membr. Sci. 566 (2018) 122–128.

[130] K. Freitag, P. Walke, T. Nilges, H. Kirchhain, R. Spranger, L. van Wüllen, Electrospun-sodiumtetrafluoroborate-polyethylene oxide membranes for solvent-free sodium ion transport in solid state sodium ion batteries, J. Power Sources 378 (2018) 610–617.

[131] G. Piana, M. Ricciardi, F. Bella, R. Cucciniello, A. Proto, C. Gerbaldi, Poly (glycidyl ether) s recycling from industrial waste and feasibility study of reuse as electrolytes in sodium-based batteries, Chem. Eng. J. 382 (2020) 122934.

[132] R. Sathiyamoorthi, R. Chandrasekaran, S. Selladurai, T. Vasudevan, Synthesis and studies of new plasticized PVP: $NaClO_3$ electrolyte system for battery applications, Ionics 9 (2003) 404–410.

[133] M.L. Lehmann, G. Yang, D. Gilmer, K.S. Han, E.C. Self, R.E. Ruther, S. Ge, B. Li, V. Murugesan, A.P. Sokolov, Tailored crosslinking of Poly (ethylene oxide) enables mechanical robustness and improved sodium-ion conductivity, Energy Storage Mater. 21 (2019) 85–96.

[134] Y. Xue, D.J. Quesnel, Synthesis and electrochemical study of sodium ion transport polymer gel electrolytes, RSC Adv. 6 (2016) 7504–7510.

[135] K. Mishra, T. Arif, R. Kumar, D. Kumar, Effect of Al_2O_3 nanoparticles on ionic conductivity of PVdF-HFP/PMMA blend-based Na^+-ion conducting nanocomposite gel polymer electrolyte, J. Solid State Electrochem. 23 (2019) 2401–2409.

[136] W. Gao, G. Du, Y. Qi, Q. Yang, W. Du, M. Xu, $Na_2TiV(PO_4)_3$@C composite with excellent Na-storage performance based on a solid-state polymer electrolyte membrane, Int. J. Energy Res. 45 (2021) 8008–8017.

[137] C.V.S. Reddy, Q.-Y. Zhu, L.-Q. Mai, W. Chen, Electrochemical studies on PVC/PVdF blend-based polymer electrolytes, J. Solid State Electrochem. 11 (2007) 543–548.

[138] N. Krishna Jyothi, K. Vijaya Kumar, G. Sunita Sundari, P. Narayana Murthy, Ionic conductivity and battery characteristic studies of a new PAN-based Na+ ion conducting gel polymer electrolyte system, Indian J. Phys. 90 (2016) 289–296.

[139] V.K. Singh, S.K. Singh, H. Gupta, Shalu, L. Balo, A.K. Tripathi, Y.L. Verma, R.K. Singh, Electrochemical investigations of Na 0.7 CoO 2 cathode with PEO-NaTFSI-BMIMTFSI electrolyte as promising material for Na-rechargeable battery, J. Solid State Electrochem. 22 (2018) 1909–1919.

[140] G. Chen, K. Zhang, Y. Liu, L. Ye, Y. Gao, W. Lin, H. Xu, X. Wang, Y. Bai, C. Wu, Flame-retardant gel polymer electrolyte and interface for quasi-solid-state sodium ion batteries, Chem. Eng. J. 401 (2020) 126065.

[141] H.C. Gao, W.D. Zhou, K. Park, J.B. Goodenough, Adv. Energy Mater. 6 (2016) 1600467.

[142] W. Li, Z.J. Yao, S.Z. Zhang, X.L. Wang, X.H. Xia, C.D. Gu, J.P. Tu, Chem. Eng. J. 423 (2021) 130310.

[143] Q. Yi, W. Zhang, S. Li, X. Li, C. Sun, Durable sodium battery with a flexible $Na_3Zr_2Si_2PO_{12}$–PVDF–HFP composite electrolyte and sodium/carbon cloth anode, ACS Appl. Mater. Interfaces 10 (41) (2018) 35039–35046.

[144] F. Colo, F. Bella, J.R. Nair, C. Gerbaldi, J. Power Sources 365 (2017) 293.

[145] J.Y. Zheng, Y.H. Zhao, X.M. Feng, W.H. Chen, Y.F. Zhao, J. Mater. Chem. A 6 (2018) 6559.
[146] S. Chen, F. Feng, Y. Yin, X. Lizo, Z. Ma, Plastic crystal polymer electrolytes containing boron based anion acceptors for room temperature all-solid-state sodium-ion batteries, Energy Storage Mater. 22 (2019) 57–65.
[147] S.L. Chen, H.Y. Che, F. Feng, J.P. Liao, H. Wang, Y.M. Yin, Z.F. Ma, ACS Appl. Mater. Interfaces 11 (2019) 43056.
[148] Y. Yang, Z. Chang, M. Li, X. Wang, Y. Wu, A sodium ion conducting gel polymer electrolyte, Solid State Ionics 269 (2015) 1–7.
[149] D. Kumar, S. Hashmi, Ionic liquid based sodium ion conducting gel polymer electrolytes, Solid State Ionics 181 (2010) 416–423.
[150] D.T. Vo, H.N. Do, T.T. Nguyen, T.T.H. Nguyen, S. Okada, M.L.P. Le, Sodium ion conducting gel polymer electrolyte using poly (vinylidene fluoride hexafluoropropylene), Mater. Sci. Eng., B 241 (2019) 27–35.
[151] K. Vignarooban, P. Badami, M. Dissanayake, P. Ravirajan, A.M. Kannan, Poly-acrylonitrile-based gel-polymer electrolytes for sodium-ion batteries, Ionics 23 (2017) 2817–2822.
[152] S. Hashmi, M.Y. Bhat, M.K. Singh, N.K. Sundaram, B.P. Raghupathy, H. Tanaka, Ionic liquid-based sodium ion-conducting composite gel polymer electrolytes: effect of active and passive fillers, J. Solid State Electrochem. 20 (2016) 2817–2826.
[153] O. Lonchakova, O. Semenikhin, M. Zakharkin, E. Karpushkin, V. Sergeyev, E. Antipov, Efficient gel-polymer electrolyte for sodium-ion batteries based on poly (acrylonitrile-co-methyl acrylate), Electrochim. Acta 334 (2020) 135512.
[154] X. Wang, Z. Liu, Y. Tang, J. Chen, Z. Mao, D. Wang, PVDF-HFP/PMMA/TPU-based gel polymer electrolytes composed of conductive $Na_3Zr_2Si_2PO_{12}$ filler for application in sodium ions batteries, Solid State Ionics 359 (2021) 115532.
[155] S. Parveen, P. Sehrawat, S.A. Hashmi, ACS Appl. Energy Mater. 5 (2022) 930.
[156] Z. Liu, X. Wang, J. Chen, Y. Tang, Z. Mao, D. Wang, Gel polymer electrolyte membranes boosted with sodium-conductive β-alumina nanoparticles: application for Na-ion batteries, ACS Appl. Energy Mater. 4 (2021) 623–632.
[157] H. Gao, B. Guo, J. Song, K. Park, J.B. Goodenough, A composite gel–polymer/glass–fiber electrolyte for sodium-ion batteries, Adv. Energy Mater. 5 (2015) 1402235.
[158] Y.B. Niu, Y.X. Yin, W.P. Wang, P.F. Wang, W. Ling, Y. Xiao, Y.G. Guo, In situ copolymerizated gel polymer electrolyte with cross-linked network for sodium-ion batteries, CCS Chem. 2 (2020) 589–597.
[159] H. Lai, Y. Lu, W. Zha, Y. Hu, Y. Zhang, X. Wu, Z. Wen, In situ generated composite gel polymer electrolyte with crosslinking structure for dendrite-free and high-performance sodium metal batteries, Energy Storage Mater. 54 (2023) 478–487.
[160] Y. Zhao, H. Liu, X. Meng, A. Liu, Y. Chen, T. Ma, A cross-linked tin oxide/polymer composite gel electrolyte with adjustable porosity for enhanced sodium ion batteries, Chem. Eng. J. 431 (2022) 133922.
[161] A.P.V.K. Saroja, A. Kumar, B.C. Moharana, M. Kamaraj, S. Ramaprabhu, Design of porous calcium phosphate based gel polymer electrolyte for quasi-solid state sodium ion battery, J. Electroanal. Chem. 859 (2020) 113864.
[162] G. Chen, K. Zhang, Y. Liu, L. Ye, Y. Gao, W. Lin, H. Xu, X. Wang, Y. Bai, C. Wu, Flame-retardant gel polymer electrolyte and interface for quasi-solid-state sodium ion batteries, Chem. Eng. J. 401 (2020) 126065.
[163] X. Wang, Z. Liu, Y. Tang, J. Chen, Z. Mao, D. Wang, PVDF-HFP/PMMA/TPU-based gel polymer electrolytes composed of conductive $Na_3Zr_2Si_2PO_{12}$ filler for application in sodium ions batteries, Solid State Ionics 359 (2021) 115532.
[164] H. Gao, B. Guo, J. Song, K. Park, J.B. Goodenough, A composite gel–polymer/glass–fiber electrolyte for sodium-ion batteries, Adv. Energy Mater. 5 (2015) 1402235.
[165] Y.B. Niu, Y.X. Yin, W.P. Wang, P.F. Wang, W. Ling, Y. Xiao, Y.G. Guo, In situ copolymerizated gel polymer electrolyte with cross-linked network for sodium-ion batteries, CCS Chem. 2 (2020) 589–597.
[166] H. Lai, Y. Lu, W. Zha, Y. Hu, Y. Zhang, X. Wu, Z. Wen, In situ generated composite gel polymer electrolyte with crosslinking structure for dendrite-free and high-performance sodium metal batteries, Energy Storage Mater. 54 (2023) 478–487.
[167] Y. Zhao, H. Liu, X. Meng, A. Liu, Y. Chen, T. Ma, A cross-linked tin oxide/polymer composite gel electrolyte with adjustable porosity for enhanced sodium ion batteries, Chem. Eng. J. 431 (2022) 133922.
[168] A.P.V.K. Saroja, A. Kumar, B.C. Moharana, M. Kamaraj, S. Ramaprabhu, Design of porous calcium phosphate based gel polymer electrolyte for quasi-solid state sodium ion battery, J. Electroanal. Chem. 859 (2020) 113864.
[169] G. Chen, K. Zhang, Y. Liu, L. Ye, Y. Gao, W. Lin, H. Xu, X. Wang, Y. Bai, C. Wu, Flame-retardant gel polymer electrolyte and interface for quasi-solid-state sodium ion batteries, Chem. Eng. J. 401 (2020) 126065.
[170] X. Wang, Z. Liu, Y. Tang, J. Chen, Z. Mao, D. Wang, PVDF-HFP/PMMA/TPU-based gel polymer electrolytes composed of conductive $Na_3Zr_2Si_2PO_{12}$ filler for application in sodium ions batteries, Solid State Ionics 359 (2021) 115532.
[171] H. Gao, W. Zhou, K. Park, J.B. Goodenough, A sodium-ion battery with a low-cost cross-linked gel-polymer electrolyte, Adv. Energy Mater. 6 (2016) 1600467.
[172] J. Shi, H. Xiong, Y. Yang, H. Shao, Nano-sized oxide filled composite PEO/PMMA/P (VDF-HFP) gel polymer electrolyte for rechargeable lithium and sodium batteries, Solid State Ionics 326 (2018) 136–144.
[173] Z. Zheng, X. Zhang, W. Shi, S. Liang, H. Cao, Y. Fu, H. Wang, Y. Zhu, AP (VDF-HFP) and nonwoven-fabric based composite as high-performance gel polymer electrolyte for fast-charging sodium metal batteries, Polymer 269 (2023) 125751.
[174] S. Janakiraman, O. Padmaraj, S. Ghosh, A. Venimadhav, A porous poly (vinylidene fluoride-co-hexafluoropropylene) based separator-cum-gel polymer electrolyte for sodium-ion battery, J. Electroanal. Chem. 826 (2018) 142–149.
[175] J. Zheng, X. Liu, Y. Duan, L. Chen, X. Zhang, X. Feng, W. Chen, Y. Zhao, Stable cross-linked gel terpolymer electrolyte containing methyl phosphonate for sodium ion batteries, J. Membr. Sci. 583 (2019) 163–170.
[176] M. Yang, F. Feng, Z. Shi, J. Guo, R. Wang, Z. Xu, Z. Liu, T. Cai, Z. Wang, C. Wang, Facile design of asymmetric flame-retardant gel polymer electrolyte with excellent interfacial stability for sodium metal batteries, Energy Storage Mater. 56 (2023) 611–620.
[177] D. Kumar, N. Yadav, K. Mishra, R. Shahid, T. Arif, D. Kanchan, Sodium ion conducting flame-retardant gel polymer electrolyte for sodium batteries and electric double layer capacitors (EDLCs), J. Energy Storage 46 (2022) 103899.
[178] J. Manuel, X. Zhao, K.-K. Cho, J.-K. Kim, J.-H. Ahn, Ultralong life organic sodium ion batteries using a polyimide/multiwalled carbon nanotubes nanocomposite and gel polymer electrolyte, ACS Sustain. Chem. Eng. 6 (2018) 8159–8166.
[179] A. Gabryelczyk, A. Swiderska-Mocek, D. Czarnecka-Komorowska, Muscovite as an inert filler for highly conductive and durable gel polymer electrolyte in sodium-ion batteries, J. Power Sources 552 (2022) 232259.
[180] X. Wang, X. Wang, J. Chen, Y. Zhao, Z. Mao, D. Wang, Durable sodium battery composed of conductive $Ti_3C_2T_x$ MXene modified gel polymer electrolyte, Solid State Ionics 365 (2021) 115655.
[181] W. Mei, X. Wang, Y. Wang, J. Chen, Z. Mao, D. Wang, Conductive $Na_3Sc_2P_3O_{12}$ filler with different crystal phases modified gel polymer electrolyte membranes for sodium ions batteries, J. Solid State Chem. 302 (2021) 122459.